




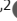








ARTICLE

Succinate-producing microbiota drives tuft cell hyperplasia to protect against *Clostridioides difficile*

Tasia D. Kellogg^{1,2,3} , Simona Ceglia^{3,4} , Benedikt M. Mortzfeld^{1,2,3} , Tanvi M. Tanna⁴ , Abigail L. Zeamer^{1,2} , Matthew R. Mancini^{1,2} , Sage E. Foley¹ , Doyle V. Ward^{1,2} , Shakti K. Bhattarai^{1,2,3} , Beth A. McCormick^{1,2,3} , Andrea Reboldi^{3,4*} , and Vanni Bucci^{1,2,3*} 

The role of microbes and their metabolites in modulating tuft cell (TC) dynamics in the large intestine and the relevance of this pathway to infections is unknown. Here, we uncover that microbiome-driven colonic TC hyperplasia protects against *Clostridioides difficile* infection. Using selective antibiotics, we demonstrate increased type 2 cytokines and TC hyperplasia in the colon but not in the ileum. We demonstrate the causal role of the microbiome in modulating this phenotype using fecal matter transplantation and administration of consortia of succinate-producing bacteria. Administration of succinate production-deficient microbes shows a reduced response in a *Pou2f3*-dependent manner despite similar intestinal colonization. Finally, antibiotic-treated mice prophylactically administered with succinate-producing bacteria show increased protection against *C. difficile*-induced morbidity and mortality. This effect is nullified in *Pou2f3*^{-/-} mice, confirming that the protection occurs via the TC pathway. We propose that activation of TCs by the microbiota in the colon is a mechanism evolved by the host to counterbalance microbiome-derived cues that facilitate invasion by pathogens.

Introduction

Microbiota-produced metabolites have a crucial role in modulating local and peripheral immune signatures (Blander et al., 2017; McCarville et al., 2020) with three prominent examples that include short chain fatty acids (SCFAs) (Arpaia et al., 2013; Atarashi et al., 2011, 2013; Foley et al., 2021; Schulthess et al., 2019; Tanoue et al., 2016), indoles (Aoki et al., 2018; Goettel et al., 2016), and secondary bile acids (Foley et al., 2022; Ridlon et al., 2014).

In the small intestine (SI), the succinate-receptor (SUCNR1) expressing taste-chemosensory epithelial tuft cells (TCs) (Lei et al., 2018) sense succinate produced by SI-specific invading parasites (Chen et al., 2022; Howitt et al., 2016; O'Leary et al., 2019) to initiate a type 2 immune signaling cascade, leading to parasite expulsion (Loke and Cadwell, 2018; Luo et al., 2019; Miller et al., 2018; Nadsombati et al., 2018; Schneider et al., 2018; von Moltke et al., 2016). TCs secrete interleukin-25 (IL-25), which induces the production of cytokines IL-4, IL-5, and IL-13 in type 2 innate lymphoid cells (Loke and Cadwell, 2018; Luo

et al., 2019; Miller et al., 2018; Nadsombati et al., 2018; Schneider et al., 2018; von Moltke et al., 2016). These type 2 cytokines act synergistically to cause hyperplasia of TCs and mucus-producing goblet cells (Schneider et al., 2018), increase SI length, increase contractility of the smooth muscle within the intestine, and recruit eosinophils to the epithelial barrier (Howitt et al., 2016). The physiological outcome of this process, referred to as the “weep and sweep” response, is the expulsion of the parasites via mucus production (weep) and increased motility (sweep) (Howitt et al., 2016; von Moltke et al., 2016).

To date, most of the literature that details the function of TCs in the gastrointestinal (GI) tract focuses on the SI and how these SI TCs interact with, respond to, and initiate protection against intestinal parasites and their substrates. Despite the interest in TCs in the GI tract and beyond, there is limited information about colonic TCs. TCs have been previously identified in the colon and shown to express SUCNR1, albeit at lower concentrations than in the ileum (Nadsombati et al., 2018; Schneider

¹Department of Microbiology, UMass Chan Medical School, Worcester, MA, USA; ²Program in Microbiome Dynamics, UMass Chan Medical School, Worcester, MA, USA; ³Immunology and Microbial Pathogenesis Program, UMass Chan Medical School, Worcester, MA, USA; ⁴Department of Pathology, UMass Chan Medical School, Worcester, MA, USA.

Correspondence to Vanni Bucci: vanni.bucci@umassmed.edu; Andrea Reboldi: andrea.reboldi@umassmed.edu

*A. Reboldi and V. Bucci are co-corresponding authors. Co-authorship and author order were determined by the recognition that the integration of the nuances of microbiome data, mathematical modeling, and immunology are different skill sets found in different laboratory environments. Each was an important component of the validity and message of this manuscript. S.E. Foley's current affiliation is Transformational and Translational Immunology Discovery Department, AbbVie, Cambridge, MA, USA.

© 2024 Kellogg et al. This article is distributed under the terms of an Attribution-Noncommercial-Share Alike-No Mirror Sites license for the first six months after the publication date (see <http://www.rupress.org/terms/>). After six months it is available under a Creative Commons License (Attribution-Noncommercial-Share Alike 4.0 International license, as described at <https://creativecommons.org/licenses/by-nc-sa/4.0/>).

et al., 2018). While some literature has demonstrated a potential impact of bacterial members of the microbiota on TCs, these papers have been limited to the SI and relied on systemic antibiotic manipulation of the microbiome (Banerjee et al., 2020). Succinate produced by the microbiota in the ileum has also been implicated in a TC-inducing model of inflammation following Paneth cell induced dysbiosis (Coutry et al., 2023). However, despite the fact that the microbiota predominantly occupies the large intestine (LI) compared with the SI by multiple orders of magnitude (Kennedy and Chang, 2020), there is, as of now, no report about communication between TCs and commensal microbes in the LI.

In the colon, succinate accumulation often occurs when the microbiome is perturbed (Tulstrup et al., 2015). It has been considered a biomarker of inflammation since higher succinate concentrations are observed in the serum and feces of inflammatory bowel disease (IBD) patients compared with healthy controls (Fremder et al., 2021). Succinate is the most prevalent biochemical route to propionate production by primary fermenters, including members of the *Bacteroides* and *Prevotella/Segatella* genera (Ikeyama et al., 2020). It is also a major cross-feeding metabolite (Fernández-Veledo and Vendrell, 2019), which was shown to enhance the *in vivo* growth of *Clostridioides difficile* (Ferreira et al., 2014), and acts as an environmental signal to regulate *Salmonella*'s virulence as well as host invasion programs (Spiga et al., 2017).

Type 2 immunity, a hallmark response to helminths and allergens, also mediates tissue regeneration in many mucocutaneous barriers, including the colon (Akdis et al., 2020; Cox et al., 2021; Gieseck et al., 2018). In mice, intraperitoneal administration of recombinant IL-25 resulted in eosinophil-mediated protection against *C. difficile* morbidity and mortality, with no effect on intestinal *C. difficile* bacterial load (Buonomo et al., 2016). Similar findings were obtained in humans with lower IL-25 concentrations found in colonic biopsies of *C. difficile*-infected patients compared with healthy controls (Buonomo et al., 2016). Finally, TCs and TC-derived IL-25 were protective in a mouse model of dextrane sulfate sodium-induced colitis (Qu et al., 2015), and patients with IBD displayed fewer IL-25-expressing cells in their intestinal mucosa, with IL-25 concentrations being lower during active disease compared with remission (Su et al., 2013). Thus, TC response is critical to maintaining homeostasis of the colonic tissue in many inflammatory and auto-inflammatory conditions, suggesting distinct TC function according to anatomy (i.e., colon versus ileum), possibly imprinted by host and environmental cues.

Here, we hypothesize that microbially produced succinate is a metabolite at the center of a three-way circuit that includes the microbiome, *C. difficile*, and host epithelial cells. Specifically, we propose that colonic TC hyperplasia in response to the accumulation of microbiota-produced succinate acts as a protective mechanism by which the host resolves *C. difficile*-related intestinal disease. Through a combination of selective microbiome disruption and supplementation experiments with antibiotics, fecal microbiota transplantation (FMT), and administration of defined microbial consortia, we demonstrate that TC hyperplasia in the colon and production of type 2 cytokines crucially

depends on colonization by succinate-producing microbes and the presence of the transcription factor *Pou2f3*, which is crucial for the differentiation of doublecortin-like kinase protein 1 (DCLK1)⁺ TCs. We further demonstrate that the administration of succinate-producing bacteria leads to protection against *C. difficile*-induced morbidity and mortality via this TC-activated pathway. Using *Pou2f3*^{-/-} mice and succinate-production knockout bacterial strains, we finally confirm that protection from *C. difficile* pathogenesis is mediated through microbiota-produced succinate-dependent colonic TC hyperplasia.

Results

Vancomycin treatment causes an increase in colonic IL-25, IL-13, IL-5, and TC number

The antibiotic vancomycin targets Gram-positive bacteria, including many succinate-consuming commensal *Clostridia* (Isaac et al., 2017), and has been shown to increase IL-25 production preferentially and specifically in the colon (Tulstrup et al., 2015; Li et al., 2019). Consequently, we hypothesized that vancomycin would globally promote type 2 cytokine production (IL-25, IL-5, IL-13) in the colon and drive TC hyperplasia. To test this, we compared tissues from mice selectively administered with either vancomycin, metronidazole, an antibiotic cocktail (ampicillin, vancomycin, neomycin, and metronidazole; AVNM), or untreated (sterile phosphate-buffered saline, PBS) for 7 days by oral gavage. We assessed the differences in IL-25, IL-13, and IL-5 concentrations by first using enzyme-linked immunosorbent assays (ELISA) (see Materials and methods). We found higher colonic IL-25 protein concentrations in vancomycin-treated mice compared with untreated (False Discovery Rate [FDR]-adjusted P value for ANOVA with Tukey post-hoc test = 0.001), AVNM-treated (P = 0.001), and metronidazole-treated (P = 0.001) mice (Fig. 1 A). Concentrations of IL-5 and IL-13 protein were also significantly elevated in the colon of vancomycin-treated mice compared to untreated, metronidazole-treated, or AVNM-treated mice (P < 0.05) (Fig. S1). Interestingly, no increase in IL-25, IL-13, or IL-5 was observed in the cecum or the ileum (Fig. S1), suggesting an anatomically compartmentalized effect of vancomycin. These initial results drove our interest specifically to the behavior of colonic TCs interacting with the microbiota. Reverse transcription-quantitative polymerase chain reaction (RT-qPCR) performed on a subset of samples recapitulated the IL-25 results. Colonic IL-25 expression was significantly increased in vancomycin-treated mice (P = 0.001) compared with mice that received PBS (e.g., untreated) or metronidazole (P = 0.01) (Fig. 1 B). We then evaluated TC hyperplasia by assessing the ratio of DCLK⁺ expressing epithelial cells relative to the number of epithelial (EPCAM⁺) cells via flow cytometry (von Moltke et al., 2016) (Fig. 1 C and Fig. S2) (see Materials and methods) and confirmed flow results via immunohistochemistry (IHC) staining of DCLK1-expressing cells (Fig. 1 D). Mice treated with vancomycin showed significantly higher proportions of TCs in the colon by flow cytometry compared with mice receiving PBS (P = 0.005) and a marginally significant increase compared with metronidazole (Fig. 1 C). Similarly, IHC showed that vancomycin-treated mice showed a

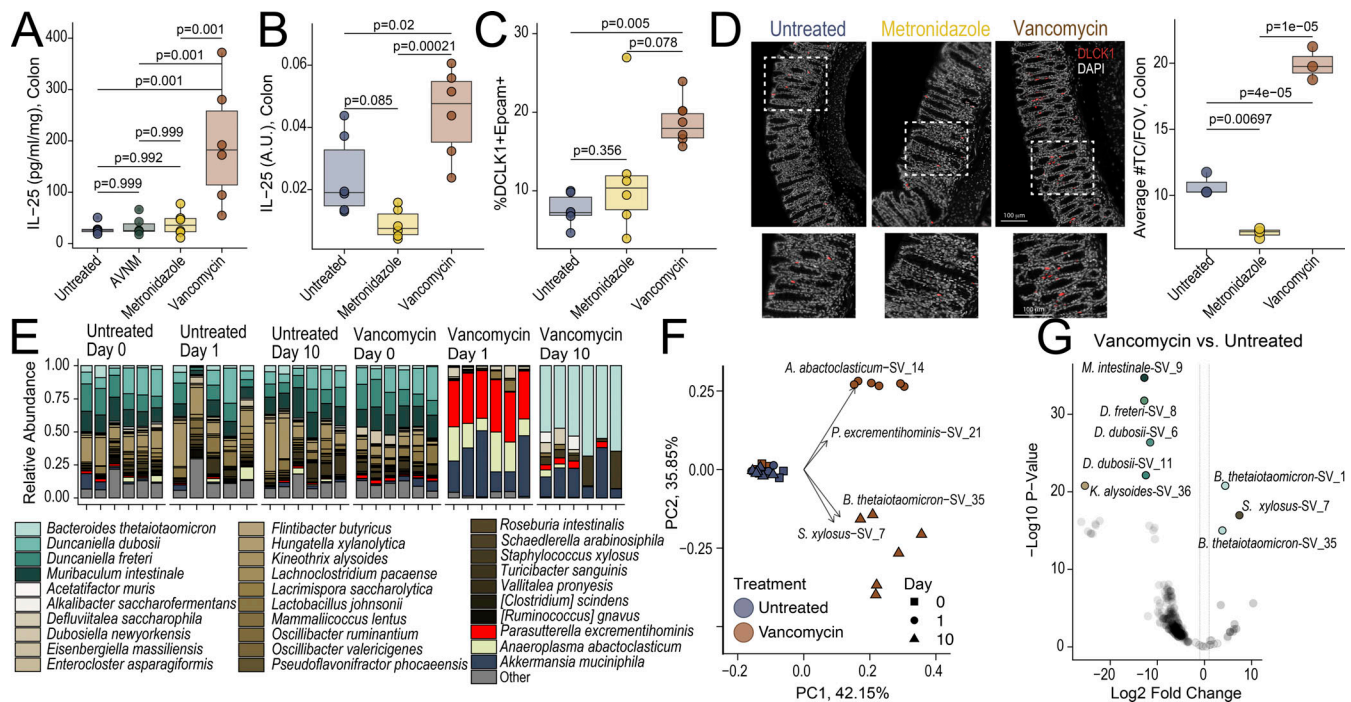


Figure 1. Vancomycin administration results in tuft cell hyperplasia and increased IL-25 concentrations in the proximal colon and leads to the enrichment of *B. thetaiotaomicon* in the microbiome. (A) Following the approach from Buonomo et al. (2016) IL-25 was measured by ELISA in the proximal colon of C57BL/6 WT mice treated with various antibiotics via oral gavage. Protein concentration in the lysate (pg/ml) was normalized by total protein in the sample (in mg) as in Buonomo et al. (2016). Data are representative of independent experiments repeated twice, using $n = 4-6$ female mice per treatment group. ANOVA with Tukey post-hoc test was run to determine significant differences. Statistical significance was estimated at FDR of 0.05. (B) IL-25 mRNA expression was measured by RT-qPCR in the proximal colon of C57BL/6 WT mice treated with different antibiotics. Data are representative of independent experiments repeated twice using $n = 4-6$ female mice per treatment group. ANOVA with Tukey post-hoc test was run to determine significant differences. Statistical significance was estimated at an FDR of 0.05. (C) TC percentages were estimated by quantifying the percentage of DCLK1⁺ EPCAM⁺ cells compared with total cells in C57BL/6 WT mice treated with various antibiotics or untreated. Data are representative of independent experiments repeated twice, using $n = 4-6$ female mice per treatment group. ANOVA with Tukey post-hoc test was run to determine significant differences. Statistical significance was estimated at FDR of 0.05. (D) TC hyperplasia was confirmed via IHC by enumerating the number of DCLK1-expressing cells in the field of view (FOV). The white bar indicates a scale of 100 μ m. Data are representative of independent experiments repeated twice, using $n = 4-6$ female mice per treatment group. ANOVA with Tukey post-hoc test was run to determine significant differences. Statistical significance was estimated at an FDR of 0.05. (E) Fecal pellets from vancomycin-treated mice and untreated mice were profiled for microbial composition via 16S rRNA sequencing at day 0, 1 and 10 after antibiotic treatment and showed enrichment in *B. thetaiotaomicon* in the samples after vancomycin treatment. (F) Principal coordinate analysis of Bray-Curtis distance demonstrates sample segregation according to antibiotic treatment and (vancomycin versus PBS) and treatment time (Day 0, 1, 10). The top four informative component loadings are shown as arrows, each represented by a corresponding microbiome SV. (G) Differential analysis for samples at day 10 was performed using DESeq2 and indicates a statistically significant enrichment of *B. thetaiotaomicon* (SVs) and *S. xylosum* in vancomycin-treated mice compared to untreated. Significance was determined based on FDR of 0.05. Note: Animals assigned to different antibiotic treatments were first co-housed to homogenize the microbiome and then separated according to treatment.

higher number of DCLK1-expressing cells compared with those treated with metronidazole or left untreated (Fig. 1 D). The observed phenotype was independent of intestinal colonization by fungi, a potential succinate producer (Begum et al., 2022), as confirmed by treatment with the antifungal amphotericin B (see Materials and methods), which resulted in no change to the enhanced IL-25, IL-13, and IL-5 protein concentrations in vancomycin-treated animals (Fig. S3). We performed 16S ribosomal RNA (16S rRNA) sequencing of fecal pellets from vancomycin-treated mice before (Day 0), during (Day 1), and at the end (Day 10) of vancomycin treatment and of fecal pellets from corresponding time points in PBS-treated mice (Fig. 1 E). Principal coordinate analysis revealed distinct sample separation based on treatment (PC1) and the timing of treatment for vancomycin-treated mice (PC2) (Fig. 1 F). Utilizing DeSeq2 for differential analysis (Love et al., 2014), we identified an

enrichment of amplicon sequencing variants (SVs) associated with succinate-producing *Bacteroides thetaiotaomicon* and *Staphylococcus xylosum* in vancomycin-treated mice compared with untreated controls (Fig. 1 G). Our findings demonstrate that vancomycin administration leads to an elevation in IL-25, IL-13, and IL-5 concentrations and TC hyperplasia in the proximal colon. This correlation coincides with the enrichment of the succinate-producer *B. thetaiotaomicon* in the microbiome.

Microbiome reconstitution with fecal matter transplant (FMT) enriched in succinate-producing bacteria increases IL-25, IL-13, and IL-5 in the colon but not in the cecum or ileum

To demonstrate the causal role of the microbiome in inducing colonic IL-25, IL-13, and IL-5, we performed FMT experiments as previously described (Ubeda et al., 2013). Mice were either treated with AVNM *ad libitum* in drinking water for 7 days or left

untreated (sterile PBS). After antibiotic treatment, mice were orally administered a pooled stool fraction obtained from mice subjected to 1 wk of vancomycin treatment; vancomycin treatment was discontinued 24 h before donor feces collection. An FMT from mice left untreated was used as the control. We observed a significant increase in the colonic concentrations of IL-25 and IL-5 (FDR-adjusted P value for ANOVA with Tukey post-hoc < 0.05) and a marginally significant increase in IL-13 ($P = 0.09$) in AVNM-treated mice receiving vancomycin-treated FMT compared to untreated FMT (Fig. 2 A). No difference was observed in mice that were not AVNM-treated (Fig. 2 A). No significant difference in IL-25 was observed in the cecum or the ileum between mice receiving vancomycin-treated FMT or untreated FMT irrespective of the treatment background (Fig. 2 B), suggesting that this microbiome-dependent induction is location-dependent. This prompted our subsequent experiments to focus on colonic TCs and compare them to SI (specifically ileal) TCs previously described in the literature to be responsive to the microbiome.

To determine differences in the microbiome of mice that differentially responded to the FMTs, we performed 16S rRNA sequencing of fecal samples obtained 24 h after the final FMT. Echoing the findings from the selective microbiome depletion experiment (Fig. 1, D–F), the FMT input from vancomycin-treated mice exhibited a dominance (>50%) of *B. thetaiotaomicro*n, which was successfully transferred to AVNM-treated mice receiving vancomycin FMT (Fig. 2 C). No significant differentially-abundant species were observed after transplant in mice receiving FMT from vancomycin-treated mice or untreated mice if they did not receive prior treatment with AVNM (FDR adjusted P value >0.05 using DeSeq2, see Love et al., 2014). This is expected, as either perturbed or naturally dysbiotic microbiotas are needed to facilitate colonization by FMT-derived bacteria (Suez et al., 2018). For the mice that received AVNM treatment, SVs belonging to succinate-producing species of *B. thetaiotaomicro*n and *Enterococcus faecalis* (Catlett et al., 2020; Kim et al., 2016) were observed to be significantly increased in relative abundance in mice receiving FMT from vancomycin-treated relative to those receiving FMT from untreated mice (Fig. 2 D) ($P < 0.05$ using DeSeq2, see Love et al., 2014). To identify which bacterial species were associated with the observed host induction in the AVNM-treated mice, we took advantage of random forest regression (RFR) modeling as we have previously described (Wipperfurth et al., 2021). Specifically, we used RFR to predict the concentration of IL-25 in every sample as a function of the abundances of all detected SVs in these mice (See Materials and methods). SVs mapping to *B. thetaiotaomicro*n and *E. faecalis* were found to be the only two bacteria (Fig. 2 E) whose increase in abundance predicts a significant increase in colonic IL-25 concentration. Positive significant associations between the abundance of *B. thetaiotaomicro*n and *E. faecalis* SVs and colonic IL-25 concentration were corroborated by running Elastic Net as well as Bayesian Variable Selection Linear Regression modeling on this data (Fig. 2 F and Fig. S4). Taken together, these data show that microbiome reconstitution with stool fractions leading to the enrichment in succinate-producing bacteria such as *B. thetaiotaomicro*n

coincides with the elevation of IL-25 and type 2-associated cytokines in the colon.

Microbiome reconstitution with defined bacteria consortia of succinate-producing strains increases IL-25, IL-13, and IL-5 in the colon but not in the cecum or ileum

The data from the FMT experiments provides causal evidence of the microbiome in promoting TC-dependent cytokine production in the colon. To demonstrate that this effect can be recapitulated by administration of a limited consortium of bacteria actively producing succinate, we first performed reconstitution experiments where AVNM-treated mice were re-colonized with either a consortium of three known *in vivo* succinate-producing *Bacteroides* and *Segatella/Prevotella* species (*B. thetaiotaomicro*n, *Bacteroides vulgatus*, and *Segatella/Prevotella copri*) (Ferreira et al., 2014; Iljazovic et al., 2021; Louis and Flint, 2017), a consortium of three common gut bacteria with no known *in vivo* succinate production (*Eggerthella lenta*, *Eubacterium rectale*, and *Dorea formicigenerans*) or with PBS as control (see Materials and methods). Mice receiving the succinate-producing consortium showed a significantly higher colonic concentration of IL-25, IL-13, and IL-5 (two-sample *t* test P value < 0.05) compared with those receiving the non-succinate-producers (Fig. 3, A–C). As in the stool transplant experiments, we did not observe significant differences between treatments in IL-25 protein concentrations in these animals' cecum or ileum (Fig. 3, D and E). This was also associated with a significantly higher percentage of TCs in the colon of succinate-producing bacteria-recipient mice compared with those receiving the non-producing strains, as measured by flow cytometry, with no significant differences observed in the ileum (Fig. 3 F). Colonic TC hyperplasia in succinate-producing bacteria-recipient mice was validated through quantification of DCLK1-expressing cells, as assessed by IHC (Fig. 3 G). Accordingly, we performed shotgun metagenomic analysis of the intestinal compartments and found significantly higher colonization by the succinate producers species *B. thetaiotaomicro*n and *B. vulgatus* in the colon, but not in the ileum of the mice receiving producers (Fig. 3 H). Similarly, we observed colonization of the non-producers species *E. lenta* and *D. formicigenerans* in the colon, but not in the ileum of the mice receiving the non-producers (Fig. 3 H). This confirmed that the difference in host phenotype induction observed in the colon of these animals was due to colonization by the inducing bacterial strains.

We then tested whether the administration of succinate-producing bacteria significantly increased succinate concentration in the gut by performing targeted metabolomics for succinate and other microbiota-associated SCFAs from colonic content, ileal content, and fecal samples from untreated, AVNM-treated, AVNM-treated receiving FMT from vancomycin-treated mice, AVNM-treated receiving succinate-producing bacteria, AVNM-treated receiving non-succinate-producing bacteria, or AVNM-treated given vehicle (PBS) (see Materials and methods). Mice gavaged with the succinate-producing bacteria after AVNM treatment displayed significantly higher concentrations of succinate compared to mice that received non-producing microbes (two-sample *t* test $P < 0.05$) (Fig. 3 I and Fig. S5). No

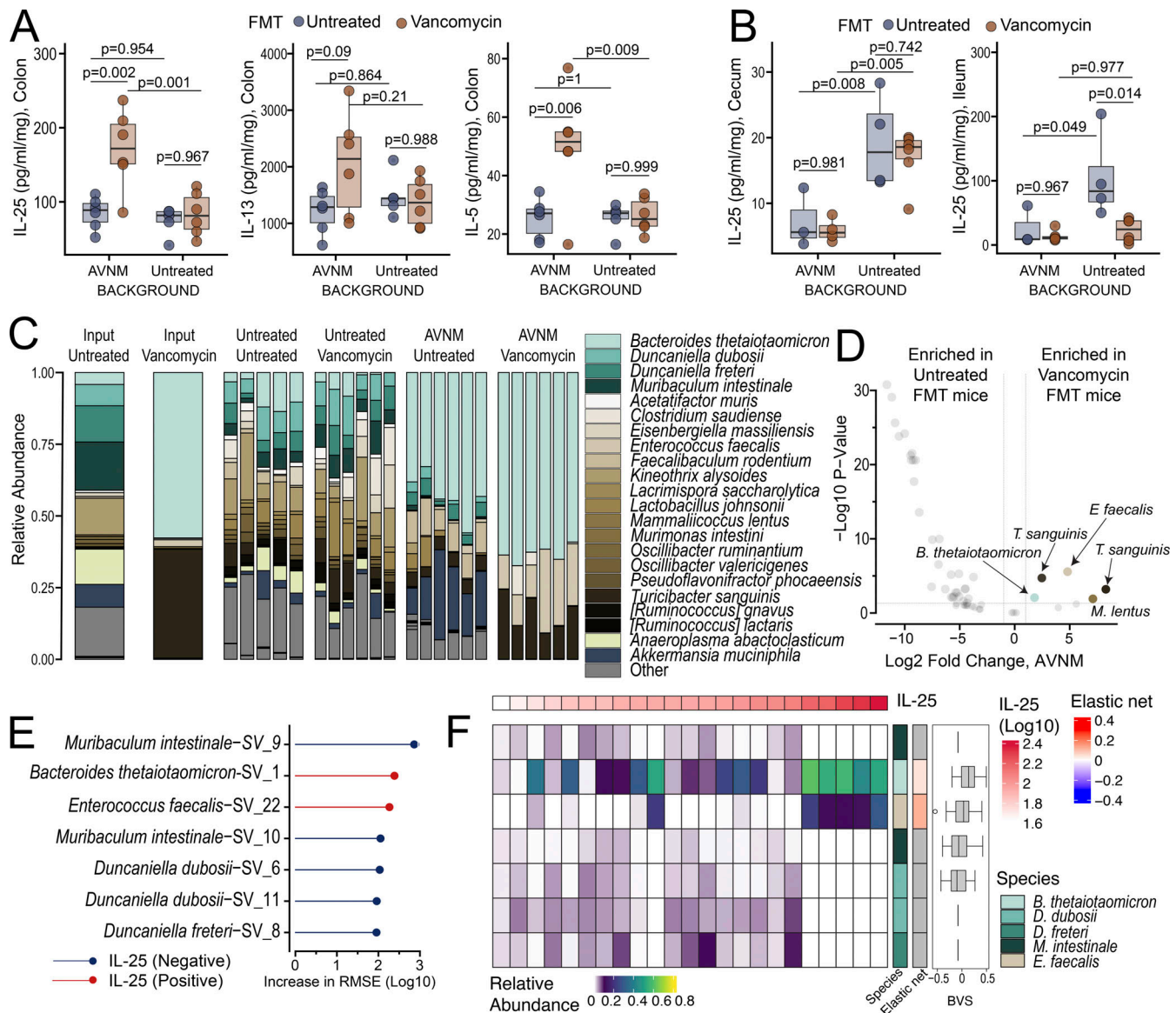


Figure 2. FMT experiments demonstrate the causal role of microbiome in the induction of type 2 cytokines in the proximal colon, which correlates with the enrichment of *B. thetaioetaomicron* in the microbiome. (A and B) IL-25, IL-5, and IL-13 concentrations were quantified in the (A) proximal colon or (B) in the ileum (for IL-25) of C57BL/6 WT mice (see Materials and methods) receiving FMTs from mice treated with vancomycin or left untreated. Prior to FMT, mice were either untreated or treated with AVNM to eliminate the resident microbiota (Background). Protein concentration in the lysate (pg/ml) was normalized by the total protein mass generated in the sample (in mg) as in [Buonomo et al. \(2016\)](#). Data are representative of independent experiments repeated twice, using $n = 4-6$ female mice per treatment group. ANOVA with Tukey post-hoc test was run to determine significant differences. Statistical significance was estimated at an FDR of 0.05. (C) 16S rRNA sequencing was conducted on input FMT and fecal samples collected from mice after FMT. (D) Volcano plots were generated following differential analysis using DeSeq2 on fecal microbiome sequencing samples from mice treated with AVNM and receiving FMT from either vancomycin-treated or untreated mice. Amplicon SVs from two succinate-producing species (*B. thetaioetaomicron* and *E. faecalis*) were found to be enriched in AVNM-treated mice receiving FMT from vancomycin-treated animals. Significance was determined based on an FDR of 0.05. (E) Permutation importance analysis followed by accumulated local effects calculations was carried out on the results of RFR modeling, which aimed to predict colonic IL-25 concentrations based on microbiome species abundance. Sequence variants associated with *B. thetaioetaomicron* and *E. faecalis* were identified as positive predictors of IL-25 concentrations in the colon. (F) The significance and directionality inferred by the RFR model were confirmed through Elastic Net Regression modeling and Bayesian Variable Selection Linear Regression. SVs linked to *B. thetaioetaomicron* and *E. faecalis* were identified as significant predictors of IL-25 accumulation in the colon. Note: Animals assigned to different FMT treatments were first co-housed based on microbiome background to homogenize the microbiome and then separated according to FMT type.

difference in succinate concentrations was detected in the ileum (Fig. 3 I), suggesting that local succinate production underpins the type 2 response and TC hyperplasia in the colon. Moreover, although several other SCFAs were enriched in mice receiving

the succinate producers compared to the non-succinate producers in the colon, they were similarly enriched in the ileum (Fig. 3 I) ruling out their association with the TC hyperplasia occurring solely in the colon.

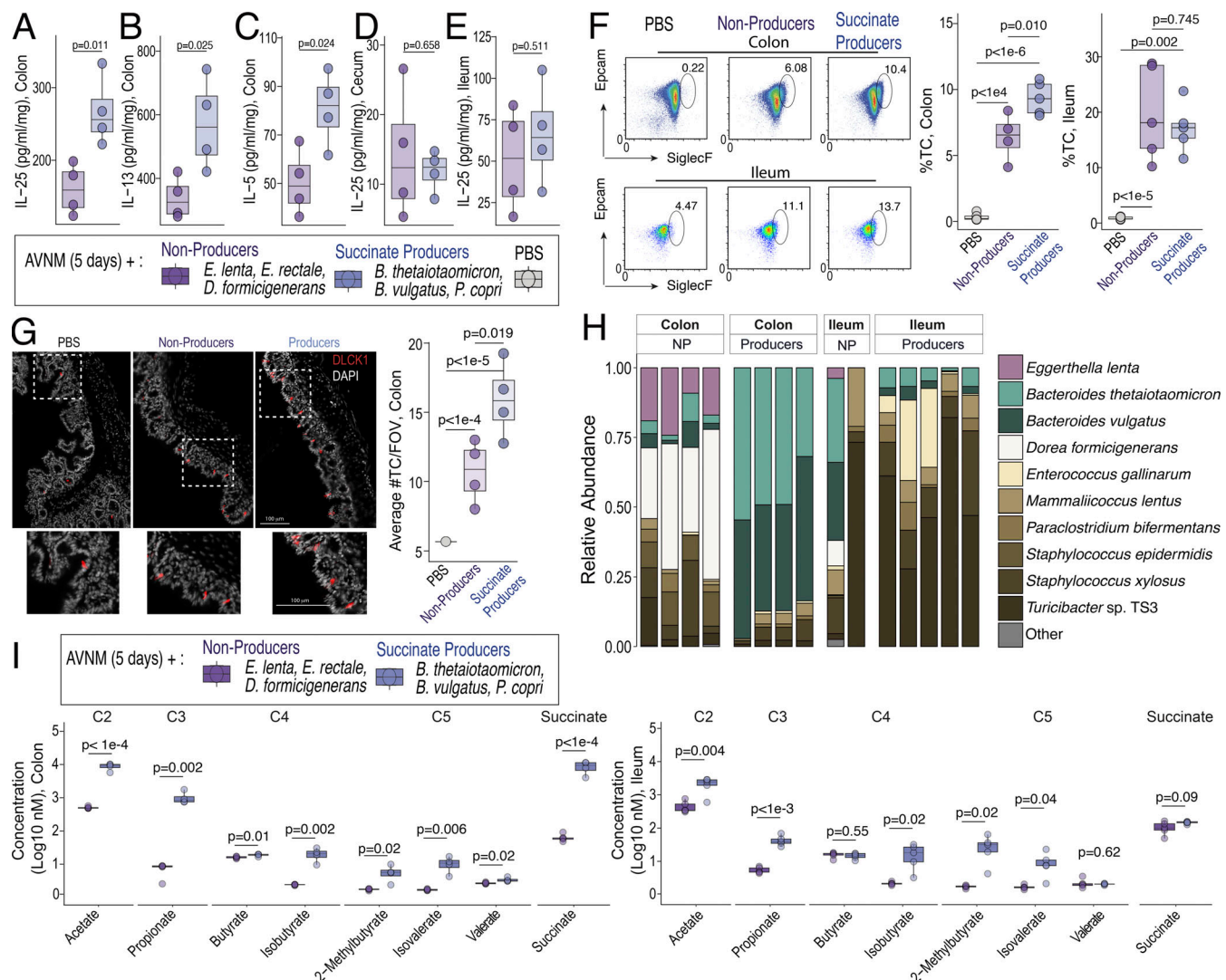


Figure 3. Consortia of succinate-producing bacteria increase colonic TCs and type 2 cytokines and corresponds to higher colonic concentrations of succinate. (A–E) IL-25, IL-13, and IL-5 protein concentrations were measured by ELISA (see Materials and methods) in the colon (D and E). IL-25 protein concentrations were also measured in the cecum and the ileum of C57BL/6 WT mice receiving succinate-producing or non-succinate-producing bacterial consortia. Protein concentration in the lysate (pg/ml) was normalized by total protein in the sample (in mg) as in [Buonuomo et al. \(2016\)](#). Data are representative of independent experiments repeated twice, using $n = 4$ female mice per treatment group. ANOVA with Tukey post-hoc test was run to determine significant differences. Statistical significance was estimated at an FDR of 0.05. **(F)** TC hyperplasia was estimated via flow cytometry in the colon and ileum of AVNM-treated C57BL/6 WT mice that were administered a consortium of three succinate producers, three succinate non-producers, or PBS. TC ratios were assessed by gating on CD45⁺Epcam⁺SiglecF⁺ cells. Data are representative of independent experiments repeated twice, using $n = 4$ –5 female mice per treatment group. ANOVA with Tukey post-hoc test was run to determine significant differences. Statistical significance was estimated at FDR of 0.05. **(G)** TC hyperplasia in the colon was confirmed via immunohistochemistry by enumerating the number of DCLK1-expressing cells in the field of view (FOV). The white bar indicates a scale of 100 μ m. Data are representative of independent experiments repeated twice, using $n = 4$ female mice per treatment group. ANOVA with Tukey post-hoc test was run to determine significant differences. Statistical significance was estimated at FDR of 0.05. **(H)** To demonstrate that phenotype induction corresponded to colonization by the bacterial consortia, we performed shotgun metagenomic sequencing. The relative abundances of the top 10 abundant species plus others are displayed as stacked bar plots and indicate colonic engraftment by the administered treatment consortia in the respective recipient mice. As expected, almost no colonization is observed in the ileum. **(I)** Targeted metabolomics was performed to quantify concentrations of acetic acid, propionic acid, butyric acid, succinic acid, 2-methylbutyric acid, isolaveric acid, valeric acid, and succinic acid in the colon and the ileum of AVNM-treated C57BL/6 WT mice receiving the succinate- or non-succinate-producing bacterial consortia. Data are representative of independent experiments repeated twice, using $n = 4$ female mice per treatment group. Two-sample t test was run to determine differentially abundant metabolites. Statistical significance was estimated at an FDR of 0.05. Note: Animals assigned to treatment with different consortia were first cohoused to homogenize the microbiome before AVNM treatment and then separated according to the type of bacterial consortium administered.

B. thetaiotaomicron emerged as the microbe most strongly associated with phenotype induction in the antibiotic treatment and fecal microbiota reconstitution experiments (Figs 1 and 2). Consequently, we aimed to verify that administering *B.*

thetaitaomicron would lead to the hyperplasia of colonic TCs. AVNM-treated animals orally gavaged with *B. thetaiotaomicron* alone showed a higher number of DCLK1-expressing cells compared with AVNM-treated animals mice administered with

heat-killed *B. thetaiotaomicron* or vehicle (PBS) (FDR-adjusted P value for ANOVA with Tukey post-hoc test <0.05) (Fig. 4 A).

We subsequently sought to confirm that succinate drives TC hyperplasia in the colon. To do this, we compared TC hyperplasia in AVNM-treated mice that were orally gavaged with either wild-type (WT) *B. thetaiotaomicron* or the succinate production-deficient *B. thetaiotaomicron* fumarate reductase knockout (Δ frd) (Spiga et al., 2017). AVNM-treated mice administered with the WT succinate-producing *B. thetaiotaomicron* displayed a significantly higher number of DCLK1-expressing cells than those administered with the *B. thetaiotaomicron* Δ frd knockout ($P < 0.05$) (Fig. 4 A). Similarly, AVNM-treated mice administered with the WT succinate-producing *B. thetaiotaomicron* showed higher percentage of TCs compared with those administered with the *B. thetaiotaomicron* Δ frd knockout or heat-killed *B. thetaiotaomicron* ($P < 0.05$) in the colon, but not in the ileum (Fig. 4 B). This also corresponded to higher concentrations of IL-25 mRNA expression (Fig. 4 C) in the colon ($P < 0.05$).

Shotgun metagenomic analysis of the colonic and ileal contents demonstrated that while both *B. thetaiotaomicron* and *B. thetaiotaomicron* Δ frd were able to colonize the colonic compartment similarly, less degree of colonization was observed in the ileum by either strain, and particularly by *B. thetaiotaomicron* Δ frd (Fig. 4 D). Similarly, metabolomics analysis in the ileum and the colon demonstrated significantly higher (FDR-adjusted P value for ANOVA with Tukey post-hoc test < 0.05) succinate concentrations in the colon of AVNM-treated mice gavaged with WT *B. thetaiotaomicron* compared with those receiving *B. thetaiotaomicron* Δ frd or heat-killed *B. thetaiotaomicron*, but not in the ileum (Fig. 4 E). Interestingly, we also observed significant differences in the concentrations of other SCFAs among the three treatments (Fig. 4 E).

To evaluate the effect that succinate production by *B. thetaiotaomicron* has on other colonic cytokines, we examined samples of inflammatory cytokines in colonic tissues by multiplexed ELISA from AVNM-treated mice orally administered with WT *B. thetaiotaomicron* or with *B. thetaiotaomicron* Δ frd. We found no differences in colonic concentrations of type 1 (IL-1b, IL-2, IL-21) and type 3 cytokines (IL-22) (two-sample *t* test $P > 0.05$) (Fig. 4 F). We found a significant reduction in type 2-associated cytokines such as IL-31 and IL-33 ($P < 0.05$) in mice gavaged with *B. thetaiotaomicron* Δ frd compared with mice gavaged with WT *B. thetaiotaomicron* (Fig. 4 G), confirming the dependency of type 2-related cytokines on *B. thetaiotaomicron*-produced succinate.

To determine if TC hyperplasia in response to *B. thetaiotaomicron*-produced succinate is intrinsic to TCs, we compared the frequency of TCs in AVNM-treated mice that were then orally gavaged with WT *B. thetaiotaomicron* or *B. thetaiotaomicron* Δ frd in C57BL/6 WT (*Pou2f3*^{+/+}), *Pou2f3*^{+/-}, and *Pou2f3*^{-/-} mice. POU2F3 is a transcription factor essential for the differentiation of DCLK1⁺ TCs throughout the body, including in the GI tract, and is implicated in the regulation of mucosal type 2 responses to helminth infection (Gerbe et al., 2016). AVNM-treated *Pou2f3*^{+/+} mice administered with WT *B. thetaiotaomicron* displayed a significantly higher percentage of TCs compared to those gavaged with *B. thetaiotaomicron* Δ frd (two-

sample *t* test P value < 0.05) in the proximal colon (Fig. 4 H). In the colon, TCs were also marginally elevated ($P = 0.104$) in AVNM-treated heterozygous mice (*Pou2f3*^{+/-}) receiving *B. thetaiotaomicron* compared to *B. thetaiotaomicron* Δ frd, but no difference was observed in the knockout mice (*Pou2f3*^{-/-}) (Fig. 4 H). Despite a genotype-dependent effect on TC abundance, with *Pou2f3*^{+/+} mice displaying more TCs compared to *Pou2f3*^{+/-} and *Pou2f3*^{-/-} in both the colon and the ileum (Fig. 4 H), no difference in TC percentages was observed between *B. thetaiotaomicron* and *B. thetaiotaomicron* Δ frd-receiving mice in the ileum. The significance of the observed genotype-dependent colonic TC hyperplasia in response to *B. thetaiotaomicron* versus *B. thetaiotaomicron* Δ frd treatment was confirmed by fitting a linear model with interaction to the TC percentages and examining the significance of the interaction coefficient ($P = 0.037$ from the model's ANOVA table, see Materials and methods). Notably, this effect was not observed in the ileum ($P > 0.05$, see Materials and methods), further emphasizing the importance of colonic colonization by *B. thetaiotaomicron* for inducing this response. Similar trends were observed when measuring IL-25 gene expression. A statistically significant elevation in IL-25 transcript was observed in the colon of *Pou2f3*^{+/+} mice when administered with *B. thetaiotaomicron* compared with *B. thetaiotaomicron* Δ frd in the colon ($P < 0.05$) but not in the ileum (Fig. 4 I). An almost total absence of expression was seen in all *Pou2f3*^{-/-} mice irrespective of the *B. thetaiotaomicron* strain administered (Fig. 4 I).

Taken together, these data provide evidence that precise microbiome supplementation with succinate-producing bacteria increases succinate concentration, TCs and type 2 cytokines in the colon, with no effect on type 1 and 3 cytokines. Additionally, the data suggest that succinate production by the microbiome is a primary driver of TC hyperplasia in the colon, where the supplemented bacteria engraft. Finally, these data highlight the importance of POU2F3 for IL-25 production in response to succinate-producing bacteria.

Prophylactic administration of succinate-producing bacteria promotes TC-mediated protection against *C. difficile*-induced morbidity and mortality

Although succinate accumulation in the lumen may promote *C. difficile* expansion in the intestine (Ferreira et al., 2014), it is unknown how this translates into host susceptibility to *C. difficile*-induced disease. Oral administration of recombinant IL-25 protects mice against *C. difficile* morbidity and mortality with no significant differences in *C. difficile* luminal CFUs (Buonomo et al., 2016). Therefore, we hypothesized that microbiome reconstitution with succinate-producing bacteria might promote colonic TC hyperplasia and initiate a succinate- and TC-dependent immune response that could culminate in protection against *C. difficile*-caused disease.

To test this hypothesis, we utilized the cefoperazone-induced *C. difficile* infection (CDI) model (Theriot et al., 2011), which we combined with our previously published approach for the adoptive transfer of *C. difficile* disease-ameliorating consortia (Buffie et al., 2015; Dsouza et al., 2022) (see Materials and methods) (Fig. 5 A). Following AVNM treatment and

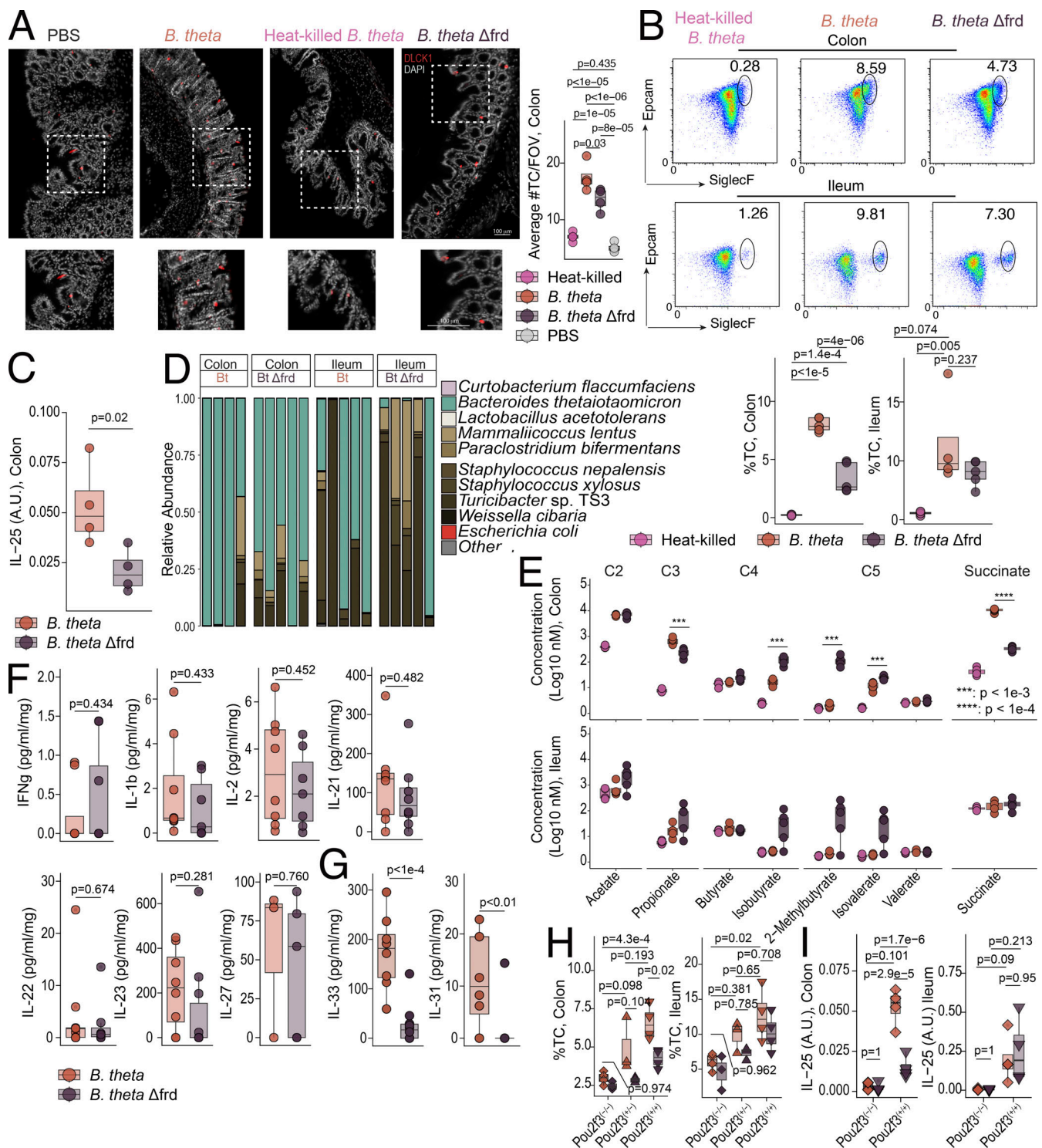


Figure 4. Colonic induction of TCs and related cytokines is dependent on the presence of succinate-producing *B. thetaiotaomicron* and Pou2f3-dependent tuft cells. AVNM-treated mice were orally gavaged with heat-killed *B. thetaiotaomicron*, live WT *B. thetaiotaomicron*, succinate production-deficient *B. thetaiotaomicron* Δ frd, or PBS. **(A)** TC hyperplasia in the colon of the mice receiving each treatment was assessed via IHC by enumerating the number of DCLK1-expressing cells in the field of view (FOV). The white bar indicates a scale of 100 μ m. Data are representative of independent experiments repeated twice, using $n = 4$ female mice per treatment group. ANOVA with Tukey post-hoc test was run to determine significant differences. Statistical significance was estimated at FDR of 0.05. **(B)** TC percentage in the colon and the ileum of AVNM-treated mice gavaged with heat-killed *B. thetaiotaomicron*, live *B. thetaiotaomicron*, or *B. thetaiotaomicron* Δ frd was evaluated via flow cytometry by gating on CD45⁺Epcam⁺SiglecF⁺ cells. Data are representative of independent experiments repeated twice, using $n = 4$ female mice per treatment group. ANOVA with Tukey post-hoc test was run to determine significant differences. Statistical significance was estimated at FDR of 0.05. **(C)** Relative mRNA expression measured by RT-qPCR of IL-25 in the proximal colon of AVNM-treated C57BL/6 WT mice treated with live *B. thetaiotaomicron* or *B. thetaiotaomicron* Δ frd. Data are representative of independent experiments repeated twice, using $n = 4$ female mice per treatment group. Two-sample t test was run to determine differentially abundant metabolites. Statistical significance was estimated at

an FDR of 0.05. **(D)** Shotgun metagenomic sequencing was performed from colonic and ileal samples to evaluate colonization by *B. thetaiotaomicron* and succinate production-deficient *B. thetaiotaomicron* Δ frd. We confirmed the engraftment of *B. thetaiotaomicron* Δ frd by mapping metagenomic reads to the *B. thetaiotaomicron* frd gene using bowtie2 and counting how many reads were mapped to frd in each treatment. **(E)** Targeted metabolomics to estimate concentrations of acetic acid, propionic acid, butyric acid, succinic acid, 2-methylbutyric acid, isovaleric acid, valeric acid, and succinic acid in the colon and the ileum of AVNM-treated C57BL/6 WT mice administered heat-killed *B. thetaiotaomicron*, *B. thetaiotaomicron* WT, or succinate production-deficient *B. thetaiotaomicron* Δ frd. Data are representative of independent experiments repeated twice, using $n = 4$ female mice per treatment group. ANOVA with Tukey post-hoc test was run to determine metabolites significantly different between treatments. Statistical significance was estimated at an FDR of 0.05. **(F and G)** Type 1, type 3, and G type 2-associated cytokines measured by Luminex Multiplex ELISA in the proximal colon of AVNM-treated C57BL/6 WT mice treated with *B. thetaiotaomicron* or *B. thetaiotaomicron* Δ frd. Data are representative of experiments repeated twice, using $n = 4$ –8 female mice per treatment group. ANOVA with Tukey post-hoc test was run to determine metabolites significantly different between treatments. Statistical significance was estimated at FDR of 0.05. **(H)** Estimation of TC percentage the colon and ileum of AVNM-treated Pou2f3^{+/-}, Pou2f3^{-/-}, and Pou2f3^{+/+} mice treated with *B. thetaiotaomicron* or *B. thetaiotaomicron* Δ frd. TC percentage was estimated via flow cytometry by gating on CD45-Epcam+SiglecF+ cells. We run ANOVA comparing the linear model with interaction, TC ~ Genotype + Treatment + Genotype:Treatment against the model with no interaction TC ~ Genotype + Treatment, to evaluate Pou2f3-dependent hyperplasia of TCs in response to different microbial treatments. Pou2f3^{+/-} and Pou2f3^{-/-} were littermates. Data are representatives of experiments repeated twice, using $n = 4$ female mice per treatment group. Pou2f3^{+/-}, Pou2f3^{-/-} were littermate, while Pou2f3^{+/+} from a different litter. Pou2f3^{+/-}, Pou2f3^{-/-}, and Pou2f3^{+/+} mice were co-housed for at least 2 wk for basal microbiome equilibration before antibiotic treatment and administration of bacteria. **(I)** Relative mRNA expression measured by RT-qPCR of IL-25 in the colon and ileum of AVNM-pretreated Pou2f3^{+/-} and Pou2f3^{+/+} mice treated with *B. thetaiotaomicron* or *B. thetaiotaomicron* Δ frd. Same modeling approach as in H was applied. Data are representatives of experiments repeated twice, using $n = 4$ female mice per treatment group. Pou2f3^{-/-} and Pou2f3^{+/+} mice were co-housed for at least 2 wk for basal microbiome equilibration before antibiotic treatment and administration of bacteria.

concurrently with cefoperazone treatment, we first administered a suspension of either the succinate-producing bacteria consortium (*B. thetaiotaomicron*, *B. vulgatus*, *S/P. copri*), a heat-killed control of the consortium, or PBS to animals prior to infection with *C. difficile* VPI 10463. Adoptive transfer of the consortium alone significantly ameliorated CDI by increasing survival (log-rank survival test P values = 0.051 and 0.014; producers versus PBS and producers versus heat-killed, respectively) (Fig. 5 B) and resulted in reduced weight loss compared with both controls (two-sample *t* test Benjamini-Hochberg adjusted P value <0.05 comparing weight loss in mice receiving producers versus PBS and mice receiving producers versus heat-killed independently at different time points) (Fig. 5 C). We measured *C. difficile* burden in the animals by quantifying the copies of the *C. difficile* toxin A (*tcdA*) gene from 100 mg of cecal content as in Kubota et al. (2014) 2 days after infection of mice gavaged with the succinate-producing consortium versus PBS. No significant difference was found between treatments (two-sample *t* test P value > 0.05) (Fig. 5 D), suggesting that the protection conferred by the succinate-producers is not due to the consortium directly impacting *C. difficile* colonization in the intestine.

To determine if the observed protection against CDI was mediated by the presence of TCs, we compared survival and weight loss in Pou2f3^{+/-} and Pou2f3^{-/-} mice that were gavaged with the consortium of succinate-producing bacteria. As hypothesized, Pou2f3^{+/-} and Pou2f3^{-/-} animals displayed increased death and weight loss compared with WT mice despite being gavaged with the succinate producers (Fig. 5, E and F). However, heterozygous Pou2f3^{+/-} mice had significantly higher survival (P = 0.008) (Fig. 5 E) and reduced weight loss compared with the homozygous Pou2f3^{-/-} (Fig. 5 F) (two-sample *t* test P < 0.05 comparing weight loss between the two genotypes). In contrast, no statistical difference in survival or weight loss due to CDI was observed between C57BL/6 wild-type and homozygous Pou2f3^{-/-} mice (Fig. 5, G and H) receiving vehicle (PBS), suggesting that the observed protection is not due to baseline genotypic differences or to other effects that are independent of the

administration of the succinate-producing bacteria. Although TC percentage is decreased in mice receiving cefoperazone compared with untreated controls (Fig. 5 I), we confirmed that C57BL/6 WT mice demonstrated a significantly higher percentage of TCs when administered with succinate-producing bacteria compared with controls immediately before *C. difficile* inoculation (FDR-adjusted P value for ANOVA with Tukey post-hoc test < 0.05), a phenomenon not observed in the Pou2f3^{-/-} background (Fig. 5 J). Interestingly, the indicated TC hyperplasia is sufficient to provide protection even though it does not return TCs to or elevate them above baseline levels. Consistent with previous experiments, treatment with succinate producers just before *C. difficile* inoculation corresponded to significantly higher succinate concentrations (P < 0.05) in the colon of C57BL/6 WT mice, but not in Pou2f3^{-/-} mice (Fig. 5 K). To demonstrate that protection was due to the succinate produced by these bacteria, we performed a cefoperazone-induced CDI experiment where C57BL/6 WT mice were orally gavaged daily for 3 days with either *B. thetaiotaomicron* or the succinate production-deficient *B. thetaiotaomicron* Δ frd. *B. thetaiotaomicron* recipient mice demonstrated significantly higher survival (Fig. 5 L) (P = 0.0044) and reduced weight loss at 48 h (P < 0.05) (Fig. 5 M) compared to the mice receiving *B. thetaiotaomicron* Δ frd. Based on our indication that *B. thetaiotaomicron* and *B. thetaiotaomicron* Δ frd achieved a similar abundance in the colon after antibiotic treatment in our animal model (Fig. 4 D), these data show that the observed difference in morbidity and mortality is due to differential succinate production by these two strains.

Altogether our data provide causal evidence that the administration of succinate-producing bacteria promotes TC hyperplasia to protect against *C. difficile*-induced morbidity and mortality. This protection is dependent on the ability of the administered bacteria to produce succinate and on the presence of Pou2f3-dependent TCs in the colon. Consistently with what was observed in Buonomo et al. (2016), the observed protection does not appear to be due to a reduced *C. difficile* titer in the intestine.

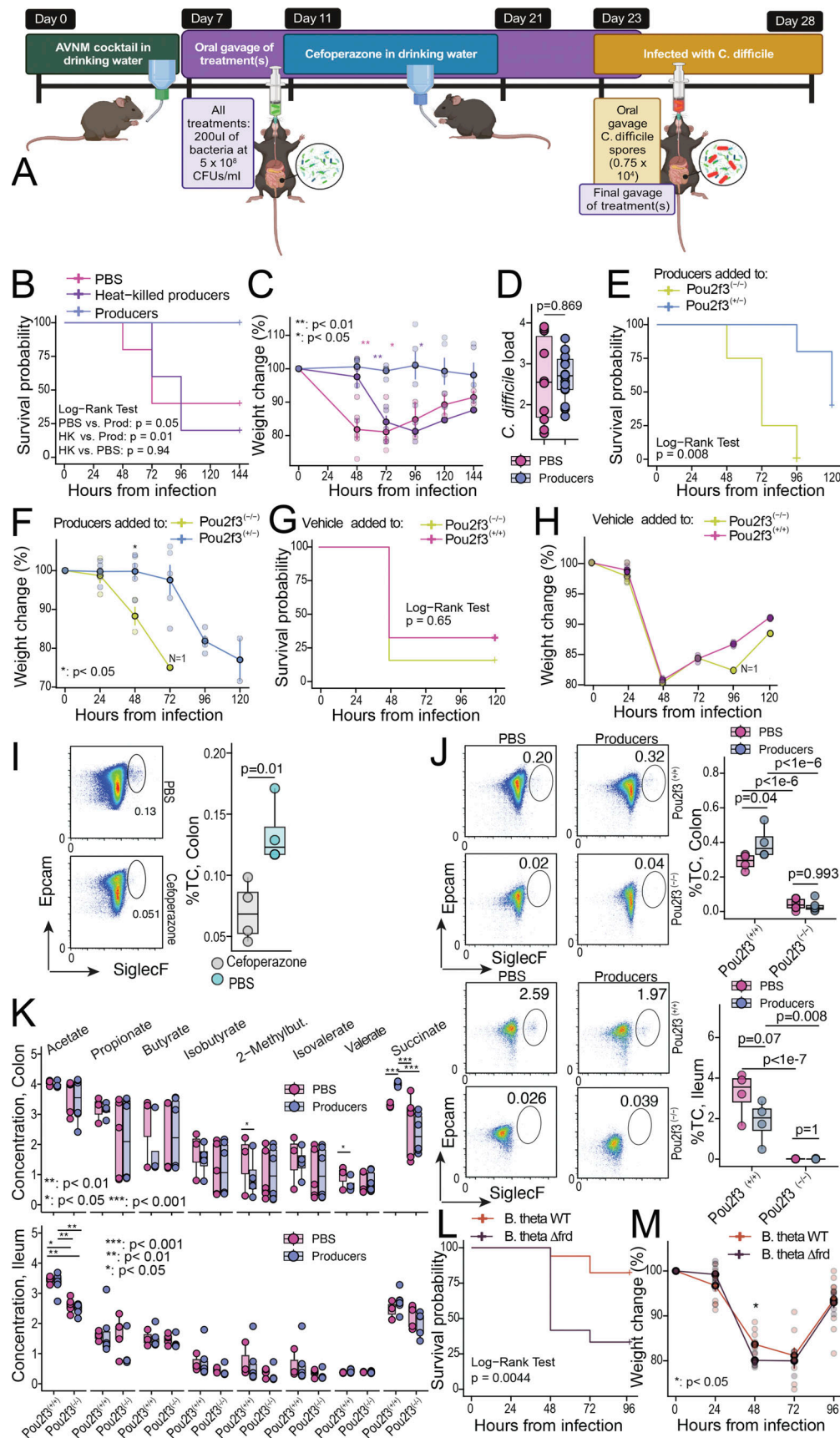


Figure 5. **Protection from *C. difficile* morbidity and mortality is achieved by prophylactic administration of succinate-producing bacteria and depends on the presence of succinate and Pou2f3-dependent TCs.** (A) Experimental diagram of the cefoperazone-based *C. difficile* infection animal model that

includes prophylactic administration of bacterial consortia and subsequent infection with *C. difficile*. **(B and C)** (B) Probability of survival and (C) change in weight compared with weight preinfection of C57BL/6 WT mice infected with *C. difficile* following treatment with a succinate-producing bacterial consortium. Representative of two independent experiments, $n = 5$ female mice per treatment. Log-rank test was performed to evaluate the difference in survival probability between each two treatments. Benjamini-Hochberg-corrected two-sample t test at different time points were performed to assess differences in weight loss between every two treatments. **(D)** Estimation of *C. difficile* toxin A (*tcdA*) titer per 100 mg of cecal content using RT-qPCR in cefoperazone-treated mice administered with succinate-producing bacterial consortium or PBS and infected with *C. difficile*, 2 days after infection; $n = 10$ female mice per treatment. Two-sample t test was performed to assess statistical significance. **(E and F)** (E) Probability of survival and (F) change in weight compared to weight preinfection of Pou2f3^{-/-} or Pou2f3^{+/-} mice infected with *C. difficile* following treatment with a succinate-producing bacterial consortium, the consortium after heat killing, or sterile PBS. Representative of two independent experiments, $n = 5$ female mice per treatment. Log-rank test was performed to evaluate difference in survival probability between each two treatments. Benjamini-Hochberg-corrected two-sample t test at different time points were performed to assess differences in weight loss between every two treatments. Pou2f3^{+/-} and Pou2f3^{-/-} were littermate cohoused after weaning. **(G and H)** (G) Probability of survival and (H) change in weight from preinfection of Pou2f3^{-/-} and Pou2f3^{+/-} mice infected with *C. difficile* following treatment with sterile PBS. Representative of two independent experiments, $n = 5$ female mice per treatment. Log-rank test was performed to evaluate difference in survival probability between each two treatments. Benjamini-Hochberg-corrected two-sample t test at different time points were performed to assess differences in weight loss between treatments. **(I)** Comparison of colonic TC numbers in C57BL/6 WT mice given cefoperazone in the drinking water versus PBS. TC percentage was evaluated via flow cytometry by gating on CD45⁻Epcam⁺SiglecF⁺ cells. Representative of two independent experiments, $n = 4$ female mice per treatment. Two-sample t test was performed to assess statistical significance. **(J)** Comparison of TC numbers in the colon and ileum of Pou2f3^{+/-} and Pou2f3^{-/-} mice administered with succinate producers or PBS immediately prior to *C. difficile* infection. Representative of two independent experiments repeated twice, $n = 4$ female mice per treatment. ANOVA with Tukey post-hoc test was run to determine differences. Statistical significance was estimated at FDR of 0.05. Pou2f3^{-/-} and Pou2f3^{+/-} mice were co-housed for at least 2 wk for basal microbiome equilibration before antibiotic treatment and administration of bacteria. **(K)** Targeted metabolomics to evaluate SCFAs and succinate concentration from colonic and ileal content from the mice of panel J. ANOVA with Tukey post-hoc test was run to determine metabolites significantly different across conditions. Statistical significance was estimated at FDR of 0.05. **(L and M)** (L) Probability of survival and (M) change in weight compared to weight pre-infection of C57BL/6 WT mice infected with *C. difficile* following treatment with *B. thetaiotaomicron* versus *B. thetaiotaomicron* Δfrd infection. Data are representative of two independent experiments repeated twice, $n = 10$ female mice per treatment. Log-rank test was performed to evaluate difference in survival probability between each two treatments. Benjamini-Hochberg-corrected two-samples t test at different time points was performed to assess differences in weight loss between treatments.

Discussion

Microbiome-produced metabolites modulate innate and adaptive immune responses in the intestine (Geva-Zatorsky et al., 2017; Zheng et al., 2020). Most mechanistic studies on this topic have focused on unveiling the causal role of microbial-derived metabolic end-products (such as SCFAs and secondary bile acids) in preserving immune homeostasis (Atarashi et al., 2011, 2013; Foley et al., 2021; Tanoue et al., 2016), and on determining the routes by which gut pathobionts promote inflammation (Atarashi et al., 2017; Britton Graham et al., 2020).

Succinate is an intermediary metabolite that is produced during the degradation of dietary fibers into other fatty acids (Fernández-Veledo and Vendrell, 2019). Succinate accumulation has been associated with a higher incidence of obesity and IBD (Serena et al., 2018), but it has also been found to promote gluconeogenesis and brain signaling (de Vadder and Mithieux, 2018). While succinate accumulation in the SI during invasion by parasites promotes the hyperplasia of TCs with implications for tissue regeneration and parasite expulsion (Ting and von Moltke, 2019; von Moltke et al., 2016), it also stimulates growth and activates virulence for different enteric pathogens such as *C. difficile* and *Salmonella* spp. (Ferreyra et al., 2014; Spiga et al., 2017). We hypothesized that colonic microbial succinate accumulation is a central signal mediating the interaction between the resident microbiota, the host, and enteric pathogens. Specifically, we hypothesized that in the absence of succinate-consuming bacteria (e.g., commensal *Clostridia* spp.), succinate accumulation is sensed by colonic TCs to initiate a program allowing the host to temporarily resist intestinal distress and pathogen-induced disease.

In support of this hypothesis, we demonstrated that selective colonic microbiome perturbation leading to the enrichment of succinate-producing microbes (through the selective depletion

of succinate consumers) induces colonic TC hyperplasia and consequent production of type 2 immune cytokines. We show the causality of the phenotype through microbiome reconstitution experiments with stool transplants that are enriched for succinate-producing bacteria, as well as by using defined consortia of known succinate-producing commensals. We demonstrate the dependency of this phenotype on microbial-produced succinate as knocking out succinate production in *B. thetaiotaomicron* leads to significantly lower TC numbers and type 2 cytokines concentrations in the colon, despite similar colonization success by the introduced strains, while not affecting concentrations of type 1 and type 3 cytokines. This effect is localized to the colon, the locus where the administered microbes engraft based on metagenomic sequencing; no effect is observed in the small intestine, corresponding to no colonization by the administered bacteria. Similarly to what was reported previously in the ileum in response to helminths infection (Gerbe et al., 2016), we importantly show that TC hyperplasia in the colon not only requires live bacteria actively producing succinate but also the TC-determining transcription factor POU2F3 as Pou2f3^{-/-} mice fail to respond.

Literature regarding cecal TC hyperplasia is still limited, with succinate receptor (SUCNR1) expression being reduced at steady state in the cecum compared with both the ileum and colon (Schneider et al., 2018). Failure to induce cecal TC hyperplasia in previous work could be due to the use of ileal-restricted helminths, or oral gavage of succinate, which is rapidly absorbed in the SI, as discussed in Hendel et al. (2022). Although it was beyond the scope of this paper to assess why cecal TCs did not respond in the same way as colonic TCs to our succinate-producing bacteria, the heterogeneity of TCs and the significantly different transcriptional and cellular profiles between the murine cecum and colon present an intriguing direction for

future research (McKinley et al., 2017; Banerjee et al., 2018; Širvinskis et al., 2022).

Following reports that exogenous administration of IL-25 protects from *C. difficile*-induced colonic damage (Buonomo et al., 2016), we show that prophylactic administration of succinate-producing live bacteria protects from *C. difficile* morbidity and mortality. Importantly, this mechanism is mediated by the presence of succinate and relies on the presence of succinate-responsive TCs, as protection is lost in *Pou2f3*^{-/-} mice. As no baseline differences in *C. difficile* mortality and morbidity in response to PBS administration are observed between *Pou2f3*^{-/-} and WT mice, the observed protection is solely due to the succinate producers-dependent hyperplasia of colonic TCs.

This is a significant advancement to studies aimed at exploiting the microbiome to control *C. difficile*-induced disease; our approach provides access to a novel microbiome-regulated axis for immune-mediated *C. difficile* control that can be complementarily explored in addition to current microbiome-based efforts at preventing *C. difficile* disease, which are focused on using bacteria intended to directly inhibit this pathogen in the intestine (Bobilev et al., 2019; Buffie et al., 2015).

Our data show that cefoperazone administration significantly decreases TC numbers in both the ileum and the colon, and that the increase of TCs by following cefoperazone with the administration of succinate-producing consortia protects from *C. difficile* disease in a *POU2F3*-dependent manner. Cefoperazone treatment is one of the main models used to induce *C. difficile* colitis in mice (Theriot et al., 2011; Winston et al., 2016). Based on our data, it is possible that cefoperazone-dependent reduction in colonic TCs occurs either by directly acting on the epithelial barrier or by (more likely) killing the resident, succinate-producing *Bacteroides* species (Erb Downward et al., 2013), and may be one of the mechanisms by which mice become susceptible to *C. difficile*. The mechanism by which cefoperazone decreases TC number remains to be elucidated; nevertheless, cefoperazone does not alter the ability of the administered microbial consortia to cause TC hyperplasia and protect from *C. difficile*. Remarkably, the succinate-producing bacterial consortia produced succinate at expected concentrations in WT and cefoperazone-treated mice, indicating that cefoperazone does not affect the ability of our gavage species to engraft in the intestine, produce succinate, and subsequently cause TC hyperplasia similarly to what is observed in AVNM-only-treated mice. Our succinate-producing consortia induce a roughly twofold increase in TCs in mice treated with cefoperazone, which subsequently provides protection against CDI despite not rescuing TC numbers to the degree observed in AVNM-treated mice gavaged with producers.

The inability of the succinate producers' administration post-AVNM to increase succinate concentrations in *Pou2f3*^{-/-} mice is intriguing as it may suggest that *Pou2f3*-dependent TCs are needed for the establishment of a succinate-producer-dominated microbiome that leads to downstream TC activation. Importantly, this observation is consistent with recent findings not only showing that mice lacking Paneth cells have a different intestinal microbiome composition in the presence and absence of TCs, but also that *Pou2f3*^{-/-} strongly negatively selects for

abundance of those same *Bacteroides* species that we found in our study to increase succinate and promote TC expansion (Coutry et al., 2023). Combined with our findings, this points to a possible, novel feedback between TCs and the microbiome that underpins intestinal response to pathogens, which has yet to be fully elucidated.

At homeostasis, succinate is a metabolic intermediate in the conversion of dietary fibers to health-promoting metabolites including SCFAs (Fernández-Veledo and Vendrell, 2019). Abnormal accumulation of microbiome-derived succinate in the intestine is a signature of gastrointestinal dysbiosis and is associated with the emergence of different diseases including IBD and obesity (Mills and O'Neill, 2014; Serena et al., 2018). Considering this, and the results of this study, we propose that succinate-sensing by colonic TCs is a sentinel mechanism that evolved to temporarily counteract the loss of succinate-to-SCFA converters during dysbiosis which may have a role in containing damage that is caused by dysbiosis-thriving opportunistic pathogens. Perhaps *C. difficile* activates virulence factors in the presence of commensal succinate to overcome the increased intestinal protection provided by TCs in the presence of a succinate-enriched microbiome.

Materials and methods

Experimental animals

All animal studies were approved by the UMass Chan Institutional Animal Care and Use Committee (Protocols A-1993-17 and PROTO202100184) in accordance with National Institutes of Health guidelines. All experiments were performed with mice 8–12 wk of age. C57BL/6J WT specific pathogen-free (SPF) mice of both sexes were purchased from The Jackson Laboratory. C57BL/6J-*Pou2f3*^{em1Cbwi/J} mice were used to generate *Pou2f*^{-/-} and *Pou2f*^{+/-} animals in-house. For all experiments involving mice purchased by external vendors, animals were acclimatized to housing facilities for at least 4 wk before their use in experiments. For the experiments in which we compared the effect of host genotype (i.e., *Pou2f*) on microbiome-dependent TC induction, we used littermate animals for *Pou2f*^{+/-} and *Pou2f*^{-/-}, while *Pou2f*^{+/+} animals were not littermate. However, in all the experiments involving mice with different genotypes, before antibiotic treatment and administration of bacterial suspensions, animals of different genotypes were first co-housed for at least 2 wk to normalize any baseline microbiome effects.

Fecal pellet collection

Mice were placed onto separate, autoclaved plastic beakers until three fecal pellets were produced. Immediately after production, individual fecal pellets were transferred using sterile toothpicks into a microfuge tube and flash-frozen in liquid nitrogen.

Antibiotic administration experiments

The approach follows previous work published by us and others (Foley et al., 2021). C57BL/6J 8–10-wk-old female SPF mice (*n* = 6–12 per treatment group, depending on the experiment) were treated with metronidazole (1 g liter⁻¹; Sigma-Aldrich), vancomycin (500 mg liter⁻¹; Sigma-Aldrich), or an antibiotic cocktail,

AVNM (a combination of ampicillin [1 g liter^{-1} ; Thermo Fisher Scientific], vancomycin [$500 \text{ mg liter}^{-1}$; Sigma-Aldrich], neomycin [1 g liter^{-1} ; Sigma-Aldrich], and metronidazole [1 g l^{-1} ; Sigma-Aldrich]) suspended in PBS or PBS as control. Each mouse received $10 \mu\text{l/g}$ bodyweight of treatment via oral gavage every 12 h for a total of 7 days. 12 h after the final antibiotic gavage, mice were sacrificed via carbon dioxide asphyxiation. Tissue samples and intestinal contents were extracted and immediately flash-frozen for immune phenotype quantification. Feces were collected before, during, and at the end of antibiotic treatment. Bacterial DNA was extracted through microbiome sequencing analysis as detailed below.

Stool matter transplant experiments

8–10-wk-old C57BL/6J female SPF mice ($n = 5\text{--}6$ per treatment group) classified as recipients were either treated with AVNM in their drinking water for 7 days to deplete the resident microbiome (Foley et al., 2021) or left on standard acidified drinking water. SPF mice ($n = 4$ per group) classified as donors were treated with vancomycin ($500 \text{ mg liter}^{-1}$; Sigma-Aldrich) or standard acidified drinking water. After 7 days of antibiotic treatment, all mice were returned to standard acidified drinking water for the remainder of the experiment. 24 h were allowed to pass between the removal of the antibiotics and the first fecal transplant to allow for antibiotic washout. Donor mice were placed individually in autoclaved plastic beakers until they produced three fecal pellets. Fecal pellets from donor mice in each group were pooled and collected into a 15 ml conical tube containing 5 ml PBS and resuspended. The fibrous matter was pelleted at $300 \times g$ for 5 min and removed from the fecal suspension to facilitate passage through the gavage needle. The fecal suspension from either untreated SPF mice or from mice previously treated with vancomycin was orally introduced to recipient mice at $10 \mu\text{l/g}$ bodyweight. This was repeated every day for 5 days, with donor feces collected and suspended fresh each day. 24 h after the final transplant, all mice were sacrificed by carbon dioxide euthanasia. Tissue samples and intestinal content extracts for immune phenotype quantification were collected and flash-frozen. Fecal samples collected over time, along with samples from input suspensions, were obtained for bacterial DNA extraction and microbiome sequencing.

Bacterial growth for live consortia

All bacterial work was performed in a Coy anaerobic chamber available in the UMass Chan Center for Microbiome Research. All strains were grown in BD Difco Reinforced Clostridial Media (BD 218081). All bacterial species were previously determined to have $\sim 1 \times 10^8$ colony-forming U/ml at an optical 600 nm (OD_{600}) of 1 when grown for 48 h. Bacterial strains were grown in 20 ml of media in sterile, anaerobic media bottles at 37°C at 50 RPMs for 48 h. OD_{600} was determined, and individual strains were pelleted at $10,000 \times g$ for 10 min. Bacterial pellets were resuspended in the appropriate volume of anaerobic, sterile PBS to produce 3.33 ml of the strain at an OD_{600} of either 1 or 5. Bacteria were then pooled to produce the consortia into either a consortium of bacteria known to produce succinate in vivo, (*B. thetaiotaomicron* VPI 5482, *B. vulgatus* NCTC 11154, and

Prevotella/S. copri DSM 18205) or a consortium of bacteria not known to produce succinate in vivo (*E. lenta* DMS2243, *E. rectale* ATCC 33656, and *D. formicigenerans* ATCC2 7755), so that the final volume of each consortium was 10 ml. The consortia were transported in anaerobic jars to ensure viability. This process was repeated daily for each administration of the live consortia. This same approach was used for the experiments comparing immune induction by *B. thetaiotaomicron* VPI 5482 and the succinate production-deficient *B. thetaiotaomicron* Δfrd (Spiga et al., 2017).

Live consortia administration experiments

8–10-wk-old C57BL/6J female SPF mice ($n = 4\text{--}8$ per treatment group, depending on the experiment) were treated with AVNM with 2% sucrose in their drinking water for 7 days to deplete the resident microbiome (see above). Mice were then administered via oral gavage either (1) “succinate-producers” described above, (2) “non-producers” described above, or (3) the succinate-producers after heat-killing for 5 min at 65°C at an OD_{600} of 1. Mice were gavaged at $10 \mu\text{l/g}$ of body weight. The gavage was repeated every 24 h for 4 days. 24 h after the last gavage of the live consortia, mice were euthanized by carbon dioxide asphyxiation. Tissue samples and intestinal extracts were collected and flash-frozen. Bacterial DNA was collected from luminal contents of the ileum and proximal colon and sequenced via shotgun metagenomics (see below). Ileal and colonic content was also subjected to targeted metabolomics (see below). The same experimental protocol and assay were used in the assays comparing phenotype induction by *B. thetaiotaomicron* VPI 5482 or the succinate-production-deficient *B. thetaiotaomicron* Δfrd (Spiga et al., 2017) in C57BL/6J, *Pou2f3*^{+/-} and *Pou2f3*^{-/-}, 8–10-wk-old female SPF mice.

C. difficile infection experiments

We evaluated the response of mice receiving different live bacterial consortia to CDI by adapting the animal model described in Theriot et al. (2011); Winston et al. (2016). 8–10-wk-old C57BL/6J female SPF mice ($n = 6$ per treatment group) were treated with sterile AVNM with 2% sucrose for 1 wk (Days 24–17 prior to infection) in their drinking water (see above). Mice were removed from AVNM and returned to standard drinking water 24 h before microbiota gavage to allow antibiotic washout. Mice were orally gavaged once every 24 h by the succinate-producers (see above) or heat-killed producers at an OD_{600} of 5 ($\sim 5 \times 10^8$ CFUs/ml), or PBS daily for 3 days at 0.2 ml/g bodyweight (16, 15, and 14 days prior to infection). 3 days after the cessation of AVNM and start of bacterial administration mice were given cefoperazone (0.5 mg/ml ; MP Bioworks) in sterile PBS with 2% sucrose for 10 days (Days 13–3 prior to infection). Mice continued to receive gavage of microbial consortia or controls every other day during the 10 days of cefoperazone treatment (9, 7, 5, and 3 days prior to infection). Cefoperazone was ceased and mice were returned to standard acidified drinking water 2 days prior to infection and received daily gavage of microbial consortia every day (2 and 1 days prior to infection). On the day of infection, mice were orally gavaged with 10^5 CFUs of *C. difficile* strain VPI 10463 (43255; ATCC) ($200 \mu\text{l}$

total volume). Animals were assessed for symptoms such as inappetence (lack of appetite), diarrhea, and hunching at 12-h intervals. Animals were euthanized if they lost 20% of their initial baseline weight. Similar CDI experiments were performed where succinate-producing bacteria or PBS were orally gavaged into Pou2f3^{+/-} and Pou2f3^{-/-} 8–10-wk-old female SPF mice ($n = 5$ –6 per treatment).

Cefoperazone administration experiment

To evaluate the intestinal epithelial effect of cefoperazone on mice receiving the antibiotic, we performed only the cefoperazone administration detailed in the CDI experiment. Mice were administered cefoperazone (0.5 mg/ml; MP Bioworks) in sterile PBS with 2% sucrose for 10 days. Control mice were administered PBS with 2% sucrose. Mice were removed from cefoperazone 2 days before euthanasia to permit the antibiotic to wash out and mimic prior experimental conditions. On day 13, mice were sacrificed via carbon dioxide asphyxiation. Tissue samples from the colon and ileum were analyzed using flow cytometry.

Tissue preparation and cytokine measurement

Cecal tissue was flushed with sterile PBS and sectioned into 0.5-cm sections before flash freezing. Ileal and proximal colon tissue were manually evacuated and sectioned into 0.5-cm sections before flash freezing. Protein lysates from intestinal tissue were generated as described in [Foley et al. \(2021\)](#) (i.e., benchtop homogenization in tubes containing Lysing Matrix D (MP Bio-medical) beads and lysis buffer (20 mM Tris pH 7.4, 120 mM NaCl, 1 mM EDTA, 1% Triton-X-100, 0.5% sodium deoxycholate, 1× protease inhibitor cocktail [Roche])). Cytokine protein concentrations were measured by ELISA (IL-17E, IL-5, and IL-13 Duo-Set; R&D Systems). Following [Buonomo et al. \(2016\)](#), cytokine protein concentration in the lysate (pg/ml) was normalized by the total protein mass generated in the sample quantified using the BioRad DC assay (in mg). RNA from epithelial cells and tissue was isolated by following the TRIzol extraction manufacture protocol. Total RNA was used for RT-qPCR. Complementary DNA was generated using iScript Reverse Transcription Supermix (catalog no. 18080-044; Invitrogen). For RT-qPCR, cDNA was mixed with appropriate primers (Table S1) and SYBR green master mix (catalog no. 1708882; BioRad) and run on a Thermocycler T100 (BioRad). Proximal colon lysates were used to measure concentrations of IL-1b, IL-2, IL-21, IL-22, IL-31, and IL-33 cytokines with multiplexed-ELISA assay with Luminex 200 Multiplex Bio-Plex 200 System (EMD Millipore) using a Milliplex Map kit (EMD Millipore).

IHC for TC quantitation

Colon and ileum were fixed overnight in 4% of PFA, followed by 2 h of washing in phosphate buffer solution and overnight incubation at 4°C in a solution of 30% sucrose. Tissues were embedded in an optimum cutting temperature compound and cut into 7-mm sections using a Leica Cryostat Microtome. Then, sections were blocked with specific serum and 5% BSA and stained with anti-DCLK1 (ab31704; Abcam), anti-CD326 (clone G8.8; BioLegend), and DAPI. Incubations were performed in Tris-buffered saline containing 5% BSA, 10% normal mouse

serum, and 0.1% Triton X-114. Sections were mounted in Fluoromount-G (catalog no. 0100-01; Southern Biotech) and imaged on a Zeiss fluorescent microscope using a ×20 objective with a numerical aperture of 0.8.

Succinate and SCFAs measurement

Quantitation of C2 to C6 SCFAs and succinic acid was carried out as previously described in [Han et al. \(2015\)](#) by the UVic-Genome BC Proteomics Centre. Briefly, serially diluted standard solutions of SCFAs and succinic acid were prepared with the use of their standard substances in 60% acetonitrile. An internal standard (IS) solution of the isotope-labeled version of SCFAs and succinic acid was prepared using 13C6-3-nitrophenylhydrazine and following the derivatizing procedure described in the publication. The samples were precisely weighed into 2-ml homogenizing tubes. 60% acetonitrile at 10 µl per mg of raw material was added. The samples were homogenized on an MM 400 mill mixer with the aid of two metal beads at 30 Hz for 3 min, followed by centrifugal clarification at 21,000 rpm and 5°C for 10 min. 20 µl of the clear supernatant of each sample or standard solution was mixed in turn with 80 µl of 200-mM 3-nitrophenylhydrazine solution and 80 µl of 150-mM EDC-6% pyridine solution. The mixtures were incubated at 40°C for 30 min. After the reaction, each solution was diluted 10-fold with the IS solution. 10-µl aliquots of the resultant solutions were injected into a C18 (2.1×150 mm, 1.8 µm) column to run liquid chromatography-tandem mass spectrometry with multiple reaction monitoring (LC-MS/MS MRM) on a Waters UPLC system coupled to a Sciex 4000 QTRAP mass spectrometer with negative-ion detection. The mobile phase was 0.01% formic acid in water (A) and 0.01% formic acid in acetonitrile (B) for binary-solvent gradient elution of 15–90% B over 15 min, at 40°C and 0.35 ml/min. Linear regression calibration curves were constructed with the data acquired from injections of the standard solutions. Concentrations of the detected analytes in the samples were calculated by interpolating the calibration curves with the peak area ratios measured from injections of the sample solutions.

Flow cytometry

Mouse intestines were opened longitudinally and vortexed in a 50-ml conical tube containing Hanks' balanced salt solution supplemented with 5% heat-inactivated FBS and 10 mM HEPES, pH 7.2. Epithelial cells were isolated by rotating the tissues in a predigestion medium (RPMI medium, 5% heat-inactivated FBS, 10 mM HEPES, pH 7.2, and 10 mM EDTA) for 30 min at 37°. Cells were stained with antibodies for CD326 (clone G8.8; BioLegend), CD45.2 (catalog no. 30-F11; BioLegend), anti-SiglecF (clone 1RNM44N; BioLegend), anti-DCLK1 (ab31704; Abcam), and LIVE/DEAD.

C. difficile quantification

Mice were sacrificed by carbon dioxide asphyxiation 48 h after infection with *C. difficile* and cecal contents were flash frozen. Genomic DNA was extracted from 100 mg mouse cecal contents using the Qiagen DNEasy PowerSoil Pro Kit. We performed an initial amplification of the region of *C. difficile* toxin A using the

listed primers (Table S1), and the amplification program consisted of one cycle at 98°C for 30 s and then 40 cycles at 98°C for 5 s, 62°C for 10 s, and 72°C for 15 s, with a final extension at 72°C for 5 min. The RT-qPCR protocol was performed as described in Kubota et al. (2014). We utilized the TaqMan primer-probe sets targeting *tcdA* (*tcdA*-F/R/P) as described (Table S1). RT-qPCR was performed in 384-well optical plates on an Applied Biosystems ViiA7Real-Time PCR System (Applied Biosystems). Each reaction mixture of 10 µl was composed of 5 µl of 2x SsoAdvanced Universal Probes Supermix (cat. no. 1725280; BioRad), 0.2 µM of each specific primer, 0.2 µM of the fluorescent probe, and 2.5 µl of template DNA. The amplification program consisted of one cycle at 95°C for 30 s and then 50 cycles at 95°C for 5 s and 56°C for 50 s. A standard curve was developed by extracting DNA from a culture of *C. difficile* VPI 10463 that had been serially plated for CFUs.

Microbiome sequencing and bioinformatics

Bacterial DNA was extracted from frozen fecal pellets and different intestinal compartments (ileum, cecum, and colon) with the DNeasy Powersoil Pro Kit by Qiagen according to the manufacturer's protocol. For the 16S rRNA sequencing, the bacterial 16S rRNA gene (variable regions V3 to V4) was subjected to PCR amplification using the universal 341F and 806R barcoded primers for Illumina sequencing. Using the SequelPrep Normalization kit, the products were pooled into sequencing libraries in equimolar amounts and sequenced on the Illumina MiSeq platform using v3 chemistry for 2 × 300 bp reads. The forward and reverse amplicon sequencing reads were dereplicated and sequences were inferred using dada2 (Callahan et al., 2016) as in Wiperman et al. (2021). For shotgun metagenomics, sequencing libraries were prepped using the Nextera XT DNA library prep kit and sequenced on a NovaSeq X Plus 2 × 150. We trimmed raw reads using Trimmomatic (version 0.39) and performed host decontamination using Bowtie2 (version 2.5.4) via the kneaddata pipeline (ver 0.10.0) (<https://github.com/biobakery/kneaddata>). The resulting metagenomic data was profiled for microbial abundance using MetaPhlAn (v4) (Beghini et al., 2021).

Statistical analysis of host readouts and metabolites

We conducted several statistical analyses to investigate variations in cytokine protein concentrations, gene expression, TC numbers, metabolite concentrations, mouse survival in response to CDI, and the effect of microbiome treatment on weight loss. To assess differences in cytokine protein concentrations, mRNA abundance, TC numbers from flow cytometry or IHC as well as microbial metabolites for conditions that included more than two treatment variables, we conducted an analysis of variance (ANOVA) followed by Tukey post-hoc tests (Hastie and Chambers, 1992). For comparisons that included two treatment variables, we used two-sample *t* tests (Chap, 2003b). We determined significant associations at an FDR value of 0.05. To evaluate genotype-dependent expansion of TCs in response to different microbial treatments (e.g., *B. thetaiotaomicron* versus *B. thetaiotaomicron* Δfrd) in different intestinal compartments, we run ANOVA comparing the linear model with interaction, TC ~ Genotype + Treatment + Genotype:Treatment against the model

with no interaction TC ~ Genotype + Treatment (Hastie and Chambers, 1992). To evaluate differences in mouse survival following CDI due to different treatments or mouse genotypes, we employed log-rank tests (Chap, 2003a). To investigate the impact of treatment on weight loss after CDI, we run Benjamini-Hochberg-corrected two-sample *t* test at different time points as in Dsouza et al. (2022). All statistical analyses were carried out using the “R” statistical software environment. Two-sample *t* test was run to assess differential *C. difficile* colonization in the cecum.

Statistical analysis and machine learning modeling of microbiome data

For the 16S rRNA sequencing data, differences in the abundance of DADA2-identified SVs between treatments were evaluated using DESeq2 (Love et al., 2014) in R. Briefly, SVs were first filtered to select based on a prevalence cutoff of 5% and relative abundance cutoff of 1e-4. Counts were then normalized by first estimating the size factors using the “median ratio method” with the *estimateSizeFactors* function (package DESeq2) and by then obtaining dispersion estimates for Negative Binomial Distributed data with the *estimateDispersions* function (package DESeq2). Finally, a Negative Binomial GLM model fitting returning Wald statistics (*DESeq2* function, from package DESeq2) was performed to assess significance and effect size (as Log2 Fold Change) for contrasts between pairs of treatments. Significant associations were determined at an FDR value of 0.05. Prediction of colonic IL-25 as a function of the abundance of 16S rRNA-determined SVs was performed by building and running RFR models as in Wiperman et al. (2021). Briefly, SVs were first converted to relative abundances by dividing each SV count by the total read counts in each sample. SVs were then filtered using 5% prevalence and 1e-4 relative abundance cut-off. Relative abundances of the filtered SVs in each sample were used to predict colonic IL-25 concentrations via RFR using the “R” *randomForest* function (package randomForest), with 10,000 trees and default *mtry* value. To determine the significance of the associations between ASVs and IL-25, the resulting random forest model was then input to the permuted variable importance algorithm using the *PIMP* function in R. Directionality positive/negative of the association was evaluated by performing Accumulated Local Effect calculation analysis via the *ALEPlot* function (package ALEPlot) in R with default values. Results from the RFR analysis were confirmed by running Elastic Net and Bayesian Variable Selection Linear Regression models using in-house code; see Bucci et al. (2016). Elastic Net models were fit to the data using the *glmnet* (package glmnet). The lambda parameter for glmnet was first calculated using 10-fold cross-validation for Gaussian functions. The Bayesian Variable Selection algorithm was implemented in the R Bayesian modeling environment *rjags*. We assumed that the zeroth and first-order term of the linear model to normally distributed with diffuse priors. We assumed that the selection parameter multiplying the first order term of the linear model to follow a Bernoulli distribution. For the data generated using shotgun metagenomic, microbiome profiling of intestinal contents was displayed using stacked bar plots as before (Dsouza et al., 2022).

Online supplemental material

Fig. S1 shows additional ELISA results from antibiotic administration, confirming increases in TC-associated cytokines in the colon, but not in the cecum or ileum. **Fig. S2** shows the estimation of the percentage of TCs via flow cytometry by quantifying DLK1+Epcam⁺ cells in mice treated with vancomycin, metronidazole, or PBS. **Fig. S3** reports the results from experiments showing that the antifungal amphotericin B does not change the ability of vancomycin to upregulate IL-25, IL5, and IL-13 in the proximal colon and confirms the bacterial role of this phenotype. **Fig. S4** reports Spearman's correlation analysis results between the relative abundance of microbiota ASVs and colonic IL-25 in AVNM-treated animals receiving FMT from untreated or vancomycin-treated mice. **Fig. S5** reports the results from targeted metabolomics for succinate and SCFAs from feces of mice treated with FMTs, succinate-producing bacteria, non-succinate-producing bacteria, or PBS. Table S1 reports the RT-qPCR primer sequences used in this study.

Data availability

All data generated in this study are presented in the manuscript and/or supplementary information. Any further information required for reproducing results or replicating the procedures will be made available by the corresponding author upon reasonable request. Microbiome sequencing data are deposited in the NCBI Short Read Archive (SRA) under accession number PRJNA1173230.

Acknowledgments

We would like to acknowledge Dr. Alexander Rudensky at Memorial Sloan-Kettering Cancer Center in New York, NY, USA and Dr. Michael Buchert at the Olivia Newton-John Cancer Research Institute, Heidelberg, Australia for their insightful conversation. We would like to thank Dr. Sebastian Winter at University of California at Davis for providing the *B. thetaiotaomicrodon* Δfrd strain.

V. Bucci acknowledges support from the Congressionally Directed Medical Research Programs grant PRMP W81XWH2020013 and the Bill & Melinda Gates Foundation. V. Bucci and B.A. McCormick acknowledge support from National Institutes of Health (NIH) U01AI172987 and NIH R01 AG075283. A. Reboldi acknowledges support from NIH R01 AI15572 and Kenneth Rainin Foundation Innovator Award. T.D. Kellogg acknowledges support by the NIH T32 AI007349-31. S. Ceglia acknowledges support from the American Association of Immunologists Careers in Immunology Fellowship Program and the Charles A. King Trust Postdoctoral Research Fellowship Award.

Author contributions: T.D. Kellogg: Conceptualization, Data curation, Formal analysis, Investigation, Methodology, Project administration, Resources, Validation, Visualization, Writing - original draft, Writing - review & editing, S. Ceglia: Data curation, Formal analysis, Investigation, Methodology, Validation, Visualization, Writing - review & editing, B.M. Mortzfeld: Conceptualization, Data curation, Project administration, Supervision, Writing - review & editing, T.M. Tanna: Investigation, Methodology, Validation, A.L. Zeamer: Conceptualization,

Methodology, M.R. Mancini: Investigation, S.E. Foley: Methodology, Writing - review & editing, D.V. Ward: Data curation, Resources, Software, Writing - review & editing, S.K. Bhattacharai: Data curation, Formal analysis, Resources, Software, Visualization, B.A. McCormick: Conceptualization, Funding acquisition, Project administration, Supervision, Visualization, Writing - original draft, Writing - review & editing, A. Reboldi: Conceptualization, Data curation, Formal analysis, Funding acquisition, Investigation, Methodology, Project administration, Resources, Supervision, Validation, Visualization, Writing - original draft, Writing - review & editing, V. Bucci: Conceptualization, Data curation, Formal analysis, Funding acquisition, Investigation, Methodology, Project administration, Resources, Software, Supervision, Visualization, Writing - original draft, Writing - review & editing.

Disclosures: T.D. Kellogg reported a patent to US 63/626,305 pending "Microbiome engineering to induce colonic Tuft Cell expansions protects from *C. difficile*-induced colitis." A. Reboldi reported a patent to US 63/626,305 pending "Microbiome engineering to induce colonic Tuft Cell expansions protects from *C. difficile*-induced colitis." V. Bucci reported grants from Vedanta Biosciences Inc. and personal fees from Vedanta Biosciences Inc. outside the submitted work; in addition, V. Bucci reported a patent to US 63/626,305 pending "Microbiome engineering to induce colonic Tuft Cell expansions protects from *C. difficile*-induced colitis." No other disclosures were reported.

Submitted: 8 November 2023

Revised: 26 September 2024

Accepted: 23 October 2024

References

- Akdis, C.A., P.D. Arkwright, M.C. Brügggen, W. Busse, M. Gadina, E. Guttman-Yassky, K. Kabashima, Y. Mitamura, L. Vian, J. Wu, and O. Palomares. 2020. Type 2 immunity in the skin and lungs. *Allergy*. 75:1582-1605. <https://doi.org/10.1111/all.14318>
- Aoki, R., A. Aoki-Yoshida, C. Suzuki, and Y. Takayama. 2018. Indole-3-pyruvic acid, an aryl hydrocarbon receptor activator, suppresses experimental colitis in mice. *J. Immunol.* 201:3683-3693. <https://doi.org/10.4049/jimmunol.1701734>
- Arpaia, N., C. Campbell, X. Fan, S. Dikiy, J. van der Veeken, P. deRoos, H. Liu, J.R. Cross, K. Pfeffer, P.J. Coffey, and A.Y. Rudensky. 2013. Metabolites produced by commensal bacteria promote peripheral regulatory T-cell generation. *Nature*. 504:451-455. <https://doi.org/10.1038/nature12726>
- Atarashi, K., W. Suda, C. Luo, T. Kawaguchi, I. Motoo, S. Narushima, Y. Kiguchi, K. Yasuma, E. Watanabe, T. Tanoue, et al. 2017. Ectopic colonization of oral bacteria in the intestine drives T_H1 cell induction and inflammation. *Science*. 358:359-365. <https://doi.org/10.1126/science.aan4526>
- Atarashi, K., T. Tanoue, K. Oshima, W. Suda, Y. Nagano, H. Nishikawa, S. Fukuda, T. Saito, S. Narushima, K. Hase, et al. 2013. Treg induction by a rationally selected mixture of Clostridia strains from the human microbiota. *Nature*. 500:232-236. <https://doi.org/10.1038/nature12331>
- Atarashi, K., T. Tanoue, T. Shima, A. Imaoka, T. Kuwahara, Y. Momose, G. Cheng, S. Yamasaki, T. Saito, Y. Ohba, et al. 2011. Induction of colonic regulatory T cells by indigenous Clostridium species. *Science*. 331:337-341. <https://doi.org/10.1126/science.1198469>
- Banerjee, A., E. McKinley, J. von Moltke, R. Coffey, and K. Lau. 2018. Interpreting heterogeneity in intestinal tuft cell structure and function. *J. Clin. Invest.* 128:1711-1719. <https://doi.org/10.1172/JCI120330>
- Banerjee, A., C.A. Herring, B. Chen, H. Kim, A.J. Simmons, A.N. Southard-Smith, M.M. Allaman, J.R. White, M.C. Macedonia, E.T. McKinley, et al.

2020. Succinate produced by intestinal microbes promotes specification of tuft cells to suppress ileal inflammation. *Gastroenterology*. 159: 2101–2115.e5. <https://doi.org/10.1053/j.gastro.2020.08.029>
- Beghini, F., L.J. McIver, A. Blanco-Míguez, L. Dubois, F. Asnicar, S. Maharjan, A. Mailyan, P. Manghi, M. Scholz, A.M. Thomas, et al. 2021. Integrating taxonomic, functional, and strain-level profiling of diverse microbial communities with bioBakery 3. *Elife*. 10:e65088. <https://doi.org/10.7554/eLife.65088>
- Begum, N., A. Harzandi, S. Lee, M. Uhlen, D.L. Moyes, and S. Shoaie. 2022. Host-mycobiome metabolic interactions in health and disease. *Gut Microbes*. 14:2121576. <https://doi.org/10.1080/19490976.2022.2121576>
- Blander, J.M., R.S. Longman, I.D. Iliev, G.F. Sonnenberg, and D. Artis. 2017. Regulation of inflammation by microbiota interactions with the host. *Nat. Immunol.* 18:851–860. <https://doi.org/10.1038/ni.3780>
- Bobilev, D., S. Bhattarai, R. Menon, B. Klein, S. Reddy, B. Olle, B. Roberts, V. Bucci, and J. Norman. 2019. VE303, a rationally designed bacterial consortium for prevention of recurrent *Clostridioides difficile* (C. Difficile) infection (rCDI), stably restores the gut microbiota after vancomycin (vanco)-Induced dysbiosis in adult healthy volunteers (HV). *Open Forum Infect. Dis.* 6:S60. <https://doi.org/10.1093/ofid/ofz359.130>
- Britton Graham, J., J. Contijoch Eduardo, P. Spindler Matthew, V. Aggarwala, B. Dogan, G. Bongers, L. San Mateo, A. Baltus, A. Das, D. Gevers, et al. 2020. Defined microbiota transplant restores Th17/RORγt+ regulatory T cell lineage in mice colonized with inflammatory bowel disease microbiotas. *Proc. Natl. Acad. Sci. USA* 117:21536–21545. <https://doi.org/10.1073/pnas.1922189117>
- Bucci, V., B. Tzen, N. Li, M. Simmons, T. Tanoue, E. Bogart, L. Deng, V. Yeliseyev, M.L. Delaney, Q. Liu, et al. 2016. MDSINE: Microbial dynamical systems INference engine for microbiome time-series analyses. *Genome Biol.* 17:121. <https://doi.org/10.1186/s13059-016-0980-6>
- Buffie, C.G., V. Bucci, R.R. Stein, P.T. McKenney, L. Ling, A. Gobourne, D. No, H. Liu, M. Kinnebrew, A. Viale, et al. 2015. Precision microbiome reconstitution restores bile acid mediated resistance to *Clostridium difficile*. *Nature*. 517:205–208. <https://doi.org/10.1038/nature13828>
- Buonomo, E.L., C.A. Cowardin, M.G. Wilson, M.M. Saleh, P. Pramoonjago, and W.A. Petri Jr. 2016. Microbiota-regulated IL-25 increases eosinophil number to provide protection during *Clostridium difficile* infection. *Cell Rep.* 16:432–443. <https://doi.org/10.1016/j.celrep.2016.06.007>
- Callahan, B.J., P.J. McMurdie, M.J. Rosen, A.W. Han, A.J.A. Johnson, and S.P. Holmes. 2016. DADA2: High-resolution sample inference from Illumina amplicon data. *Nat. Methods*. 13:581–583. <https://doi.org/10.1038/nmeth.3869>
- Catlett, J.L., J. Catazaro, M. Cashman, S. Carr, R. Powers, M.B. Cohen, and N.R. Buan. 2020. Metabolic feedback inhibition influences metabolite secretion by the human gut symbiont *Bacteroides thetaiotaomicron*. *mSystems*. 5:e00252–20. <https://doi.org/10.1128/mSystems.00252-20>
- Chap, L. 2003a. Analysis of survival data and data from matched studies. In *Introductory Biostatistics*. 379–444. <https://doi.org/10.1002/0471308889>
- Chap, L. 2003b. Introduction to statistical tests of significance. In *Introductory Biostatistics*. 188–207.
- Chen, J., Y. Wang, L. Shen, Y. Xiu, and B. Wang. 2022. Could IL-25 be a potential therapeutic target for intestinal inflammatory diseases? *Cytokine Growth Factor Rev.* 69:43–50. <https://doi.org/10.1016/j.cytogfr.2022.07.001>
- Coutry, N., J. Nguyen, S. Soualhi, F. Gerbe, V. Meslier, V. Dardalhon, M. Almeida, B. Quinquis, F. Thirion, F. Herbert, et al. 2023. Cross talk between Paneth and tuft cells drives dysbiosis and inflammation in the gut mucosa. *Proc. Natl. Acad. Sci. USA*. 120:e2219431120. <https://doi.org/10.1073/pnas.2219431120>
- Cox, J.R., S.M. Cruickshank, and A.E. Saunders. 2021. Maintenance of barrier tissue integrity by unconventional lymphocytes. *Front. Immunol.* 12: 670471. <https://doi.org/10.3389/fimmu.2021.670471>
- de Vadder, F., and G. Mithieux. 2018. Gut-brain signaling in energy homeostasis: The unexpected role of microbiota-derived succinate. *J. Endocrinol.* 236:R105–R108. <https://doi.org/10.1530/JOE-17-0542>
- Dsouza, M., R. Menon, E. Crossette, S.K. Bhattarai, J. Schneider, Y.-G. Kim, S. Reddy, S. Caballero, C. Felix, L. Cornacchione, et al. 2022. Colonization of the live biotherapeutic product VE303 and modulation of the microbiota and metabolites in healthy volunteers. *Cell Host Microbe*. 30: 583–598.e8. <https://doi.org/10.1016/j.chom.2022.03.016>
- Erb Downward, J.R., N.R. Falkowski, K.L. Mason, R. Muraglia, and G.B. Huffnagle. 2013. Modulation of post-antibiotic bacterial community reassembly and host response by *Candida albicans*. *Sci. Rep.* 3:2191. <https://doi.org/10.1038/srep02191>
- Fernández-Veledo, S., and J. Vendrell. 2019. Gut microbiota-derived succinate: Friend or foe in human metabolic diseases? *Rev. Endocr. Metab. Disord.* 20:439–447. <https://doi.org/10.1007/s11154-019-09513-z>
- Ferreira, J.A., K.J. Wu, A.J. Hryckowian, D.M. Bouley, B.C. Weimer, and J.L. Sonnenburg. 2014. Gut microbiota-produced succinate promotes *C. difficile* infection after antibiotic treatment or motility disturbance. *Cell Host Microbe*. 16:770–777. <https://doi.org/10.1016/j.chom.2014.11.003>
- Foley, S.E., M.J. Dente, X. Lei, B.F. Sallis, E.B. Loew, M. Meza-Segura, K.A. Fitzgerald, and B.A. McCormick. 2022. Microbial metabolites orchestrate a distinct multi-tiered regulatory network in the intestinal epithelium that directs P-glycoprotein expression. *MBio*. 13:e0199322. <https://doi.org/10.1128/mbio.01993-22>
- Foley, S.E., C. Tuohy, M. Dunford, M.J. Grey, H. De Luca, C. Cawley, R.L. Szabady, A. Maldonado-Contreras, J.M. Houghton, D.V. Ward, et al. 2021. Gut microbiota regulation of P-glycoprotein in the intestinal epithelium in maintenance of homeostasis. *Microbiome*. 9:183. <https://doi.org/10.1186/s40168-021-01137-3>
- Fremder, M., S.W. Kim, A. Khamaysi, L. Shimshilashvili, H. Eini-Rider, I.S. Park, U. Hadad, J.H. Cheon, and E. Ohana. 2021. A transepithelial pathway delivers succinate to macrophages, thus perpetuating their pro-inflammatory metabolic state. *Cell Rep.* 36:109521. <https://doi.org/10.1016/j.celrep.2021.109521>
- Gerbe, F., E. Sidot, D.J. Smyth, M. Ohmoto, I. Matsumoto, V. Dardalhon, P. Cesses, L. Garnier, M. Pouzolles, B. Brulin, et al. 2016. Intestinal epithelial tuft cells initiate type 2 mucosal immunity to helminth parasites. *Nature*. 529:226–230. <https://doi.org/10.1038/nature16527>
- Geva-Zatorsky, N., E. Sefik, L. Kua, L. Pasman, T.G. Tan, A. Ortiz-Lopez, T.B. Yanortsang, L. Yang, R. Jupp, D. Mathis, et al. 2017. Mining the human gut microbiota for immunomodulatory organisms. *Cell*. 168:928–943.e11. <https://doi.org/10.1016/j.cell.2017.01.022>
- Gieseck, R.L. III, M.S. Wilson, and T.A. Wynn. 2018. Type 2 immunity in tissue repair and fibrosis. *Nat. Rev. Immunol.* 18:62–76. <https://doi.org/10.1038/nri.2017.90>
- Goettel, J.A., R. Gandhi, J.E. Kenison, A. Yeste, G. Murugaiyan, S. Sambanthamoorthy, A.E. Griffith, B. Patel, D.S. Shouval, H.L. Weiner, et al. 2016. AHR activation is protective against colitis driven by T cells in humanized mice. *Cell Rep.* 17:1318–1329. <https://doi.org/10.1016/j.celrep.2016.09.082>
- Han, J., K. Lin, C. Sequeira, and C.H. Borchers. 2015. An isotope-labeled chemical derivatization method for the quantitation of short-chain fatty acids in human feces by liquid chromatography-tandem mass spectrometry. *Anal. Chim. Acta*. 854:86–94. <https://doi.org/10.1016/j.aca.2014.11.015>
- Hastie, T.J., and J.M. Chambers. 1992. Statistical Models. In *Statistical Models in S*. J.M. Chambers, and T.J. Hastie, editors. Wadsworth & Brooks/Cole, Pacific Grove, CA, USA. pp. 13–44. Available at: https://www.routledge.com/Statistical-Models-in-S/Chambers-Hastie/p/book/9780412830402?srsltid=AfmBOoQAY7j4z80_E0FzWtCcGyXMArMytdP7n38g7U_NSlKFGKDZs6
- Hendel, S.K., L. Kellermann, A. Hausmann, N. Bindsløv, K.B. Jensen, and O.H. Nielsen. 2022. Tuft cells and their role in intestinal diseases. *Front. Immunol.* 13:822867. <https://doi.org/10.3389/fimmu.2022.822867>
- Howitt, M.R., S. Lavoie, M. Michaud, A.M. Blum, S.V. Tran, J.V. Weinstock, C.A. Gallini, K. Redding, R.F. Margolskee, L.C. Osborne, et al. 2016. Tuft cells, taste-chemosensory cells, orchestrate parasite type 2 immunity in the gut. *Science*. 351:1329–1333. <https://doi.org/10.1126/science.aaf648>
- Ikeyama, N., T. Murakami, A. Toyoda, H. Mori, T. Iino, M. Ohkuma, and M. Sakamoto. 2020. Microbial interaction between the succinate-utilizing bacterium *Phascolarctobacterium faecium* and the gut commensal *Bacteroides thetaiotaomicron*. *MicrobiologyOpen*. 9:e1111. <https://doi.org/10.1002/mbo3.1111>
- Iljazovic, A., U. Roy, E.J.C. Gálvez, T.R. Lesker, B. Zhao, A. Gronow, L. Amend, S.E. Will, J.D. Hofmann, M.C. Pils, et al. 2021. Perturbation of the gut microbiome by *Prevotella* spp. enhances host susceptibility to mucosal inflammation. *Mucosal Immunol.* 14:113–124. <https://doi.org/10.1038/s41385-020-0296-4>
- Isaac, S., J.U. Scher, A. Djukovic, N. Jiménez, D.R. Littman, S.B. Abramson, E.G. Pamer, and C. Ubeda. 2017. Short- and long-term effects of oral vancomycin on the human intestinal microbiota. *J. Antimicrob. Chemother.* 72:128–136. <https://doi.org/10.1093/jac/dkw383>
- Kennedy, M.S., and E.B. Chang. 2020. The microbiome: Composition and locations. *Prog. Mol. Biol. Transl. Sci.* 176:1–42. <https://doi.org/10.1016/bs.pmbts.2020.08.013>
- Kim, S.H., L.L. Mamuad, D.W. Kim, S.K. Kim, and S.S. Lee. 2016. Fumarate reductase-producing enterococci reduce methane production in rumen fermentation in vitro. *J. Microbiol. Biotechnol.* 26:558–566. <https://doi.org/10.4014/jmb.1512.12008>
- Kubota, H., T. Sakai, A. Gawad, H. Makino, T. Akiyama, E. Ishikawa, and K. Oishi. 2014. Development of TaqMan-based quantitative PCR for

- sensitive and selective detection of toxigenic *Clostridium difficile* in human stools. *PLoS One*. 9:e111684. <https://doi.org/10.1371/journal.pone.0111684>
- Lei, W., W. Ren, M. Ohmoto, J.F. Urban Jr., I. Matsumoto, R.F. Margolskee, and P. Jiang. 2018. Activation of intestinal tuft cell-expressed *Sucnr1* triggers type 2 immunity in the mouse small intestine. *Proc. Natl. Acad. Sci. USA*. 115:5552–5557. <https://doi.org/10.1073/pnas.1720758115>
- Li, X., M. Mao, Y. Zhang, K. Yu, and W. Zhu. 2019. Succinate modulates intestinal barrier function and inflammation response in pigs. *Biomolecules*. 9. 486. <https://doi.org/10.3390/biom9090486>
- Loke, P., and K. Cadwell. 2018. Getting a taste for parasites in the gut. *Immunity*. 49:16–18. <https://doi.org/10.1016/j.immuni.2018.07.002>
- Louis, P., and H.J. Flint. 2017. Formation of propionate and butyrate by the human colonic microbiota. *Environ. Microbiol.* 19:29–41. <https://doi.org/10.1111/1462-2920.13589>
- Love, M.I., W. Huber, and S. Anders. 2014. Moderated estimation of fold change and dispersion for RNA-seq data with DESeq2. *Genome Biol.* 15: 550. <https://doi.org/10.1186/s13059-014-0550-8>
- Luo, X.C., Z.H. Chen, J.B. Xue, D.X. Zhao, C. Lu, Y.H. Li, S.M. Li, Y.W. Du, Q. Liu, P. Wang, et al. 2019. Infection by the parasitic helminth *Trichinella spiralis* activates a *Tas2r*-mediated signaling pathway in intestinal tuft cells. *Proc. Natl. Acad. Sci. USA*. 116:5564–5569. <https://doi.org/10.1073/pnas.1812901116>
- McCarville, J.L., G.Y. Chen, V.D. Cuevas, K. Troha, and J.S. Ayres. 2020. Microbiota metabolites in health and disease. *Annu. Rev. Immunol.* 38: 147–170. <https://doi.org/10.1146/annurev-immunol-071219-125715>
- McKinley, E., Y. Sui, Y. Al-Kofahi, B. Millis, M. Tyska, J. Roland, A. Santamaria-Pang, C. Ohland, C. Jobin, J. Franklyn, et al. 2017. Optimized multiplex immunofluorescence single-cell analysis reveals tuft cell heterogeneity. *JCI Insight*. 2. e93487. <https://doi.org/10.1172/jci.insight.93487>
- Miller, C.N., I. Proekt, J. von Moltke, K.L. Wells, A.R. Rajpurkar, H. Wang, K. Rattay, I.S. Khan, T.C. Metzger, J.L. Pollack, et al. 2018. Thymic tuft cells promote an IL-4-enriched medulla and shape thymocyte development. *Nature*. 559:627–631. <https://doi.org/10.1038/s41586-018-0345-2>
- Mills, E., and L.A. O'Neill. 2014. Succinate: A metabolic signal in inflammation. *Trends Cell Biol.* 24:313–320. <https://doi.org/10.1016/j.tcb.2013.11.008>
- Nadjsombati, M.S., J.W. McGinty, M.R. Lyons-Cohen, J.B. Jaffe, L. DiPeso, C. Schneider, C.N. Miller, J.L. Pollack, G.A. Nagana Gowda, M.F. Fontana, et al. 2018. Detection of succinate by intestinal tuft cells triggers a type 2 innate immune circuit. *Immunity*. 49:33–41.e7. <https://doi.org/10.1016/j.immuni.2018.06.016>
- O'Leary, C.E., C. Schneider, and R.M. Locksley. 2019. Tuft cells-systemically dispersed sensory epithelia integrating immune and neural circuitry. *Annu. Rev. Immunol.* 37:47–72. <https://doi.org/10.1146/annurev-immunol-042718-041505>
- Qu, D., N. Weygant, R. May, P. Chandrakesan, M. Madhoun, N. Ali, S.M. Sureban, G. An, M.J. Schlosser, and C.W. Houchen. 2015. Ablation of doublecortin-like kinase 1 in the colonic epithelium exacerbates dextran sulfate sodium-induced colitis. *PLoS One*. 10:e0134212. <https://doi.org/10.1371/journal.pone.0134212>
- Ridlon, J.M., D.J. Kang, P.B. Hylemon, and J.S. Bajaj. 2014. Bile acids and the gut microbiome. *Curr. Opin. Gastroenterol.* 30:332–338. <https://doi.org/10.1097/MOG.0000000000000057>
- Schneider, C., C.E. O'Leary, J. von Moltke, H.E. Liang, Q.Y. Ang, P.J. Turnbaugh, S. Radhakrishnan, M. Pellizzon, A. Ma, and R.M. Locksley. 2018. A metabolite-triggered tuft cell-ILC2 circuit drives small intestinal remodeling. *Cell*. 174:271–284.e14. <https://doi.org/10.1016/j.cell.2018.05.014>
- Schulthess, J., S. Pandey, M. Capitani, K.C. Rue-Albrecht, I. Arnold, F. Franchini, A. Chomka, N.E. Ilott, D.G.W. Johnston, E. Pires, et al. 2019. The short chain fatty acid butyrate imprints an antimicrobial program in macrophages. *Immunity*. 50:432–445.e7. <https://doi.org/10.1016/j.immuni.2018.12.018>
- Serena, C., V. Ceperuelo-Mallafre, N. Keiran, M.I. Queipo-Ortuño, R. Bernal, R. Gomez-Huelgas, M. Urpi-Sarda, M. Sabater, V. Pérez-Brocá, C. Andrés-Lacueva, et al. 2018. Elevated circulating levels of succinate in human obesity are linked to specific gut microbiota. *ISME J.* 12: 1642–1657. <https://doi.org/10.1038/s41396-018-0068-2>
- Širvinskis, D., O. Omrani, J. Lu, M. Rasa, A. Krepelova, L. Adam, S. Kaepfel, F. Sommer, and F. Neri. 2022. Single-cell atlas of the aging mouse colon. *iScience*. 25. 104202. <https://doi.org/10.1016/j.isci.2022.104202>
- Spiga, L., M.G. Winter, T. Furtado de Carvalho, W. Zhu, E.R. Hughes, C.C. Gillis, C.L. Behrendt, J. Kim, D. Chessa, H.L. Andrews-Polymeris, et al. 2017. An oxidative central metabolism enables *Salmonella* to utilize microbiota-derived succinate. *Cell Host Microbe*. 22:291–301.e6. <https://doi.org/10.1016/j.chom.2017.07.018>
- Su, J., T. Chen, X.Y. Ji, C. Liu, P.K. Yadav, R. Wu, P. Yang, and Z. Liu. 2013. IL-25 downregulates Th1/Th17 immune response in an IL-10-dependent manner in inflammatory bowel disease. *Inflamm. Bowel Dis.* 19:720–728. <https://doi.org/10.1097/MIB.0b013e3182802a76>
- Suez, J., N. Zmora, G. Zilberman-Schapira, U. Mor, M. Dori-Bachash, S. Bashardes, M. Zur, D. Regev-Lehavi, R. Ben-Zeev Briki, S. Federici, et al. 2018. Post-antibiotic gut mucosal microbiome reconstitution is impaired by probiotics and improved by autologous FMT. *Cell*. 174: 1406–1423.e16. <https://doi.org/10.1016/j.cell.2018.08.047>
- Tanoue, T., K. Atarashi, and K. Honda. 2016. Development and maintenance of intestinal regulatory T cells. *Nat. Rev. Immunol.* 16:295–309. <https://doi.org/10.1038/nri.2016.36>
- Theriot, C.M., C.C. Koumpouras, P.E. Carlson, I.I. Bergin, D.M. Aronoff, and V.B. Young. 2011. Cefoperazone-treated mice as an experimental platform to assess differential virulence of *Clostridium difficile* strains. *Gut Microbes*. 2:326–334. <https://doi.org/10.4161/gmic.19142>
- Ting, H.-A., and J. von Moltke. 2019. The immune function of tuft cells at gut mucosal surfaces and beyond. *J. Immunol.* 202:1321–1329. <https://doi.org/10.4049/jimmunol.1801069>
- Tulstrup, M.V., E.G. Christensen, V. Carvalho, C. Linnings, S. Ahn, O. Højberg, T.R. Licht, and M.I. Bahl. 2015. Antibiotic treatment affects intestinal permeability and gut microbial composition in wistar rats dependent on antibiotic class. *PLoS One*. 10:e0144854. <https://doi.org/10.1371/journal.pone.0144854>
- Ubeda, C., V. Bucci, S. Caballero, A. Djukovic, N.C. Toussaint, M. Equinda, L. Lipuma, L. Ling, A. Gobourne, D. No, et al. 2013. Intestinal microbiota containing *Barnesiella* species cures vancomycin-resistant *Enterococcus faecium* colonization. *Infect. Immun.* 81:965–973. <https://doi.org/10.1128/IAI.01197-12>
- von Moltke, J., M. Ji, H.E. Liang, and R.M. Locksley. 2016. Tuft-cell-derived IL-25 regulates an intestinal ILC2-epithelial response circuit. *Nature*. 529:221–225. <https://doi.org/10.1038/nature16161>
- Winston, J.A., R. Thanissery, S.A. Montgomery, and C.M. Theriot. 2016. Cefoperazone-treated mouse model of clinically-relevant *Clostridium difficile* strain R20291. *J. Vis. Exp.*:54850. <https://doi.org/10.3791/54850>
- Wipperfurth, M.F., S.K. Bhattarai, C.K. Vorkas, V.S. Maringati, Y. Taur, L. Mathurin, K. McAulay, S.C. Vilbrun, D. Francois, J. Bean, et al. 2021. Gastrointestinal microbiota composition predicts peripheral inflammatory state during treatment of human tuberculosis. *Nat. Commun.* 12: 1141. <https://doi.org/10.1038/s41467-021-21475-y>
- Zheng, D., T. Liwski, and E. Elinav. 2020. Interaction between microbiota and immunity in health and disease. *Cell Res.* 30:492–506. <https://doi.org/10.1038/s41422-020-0332-7>

Supplemental material

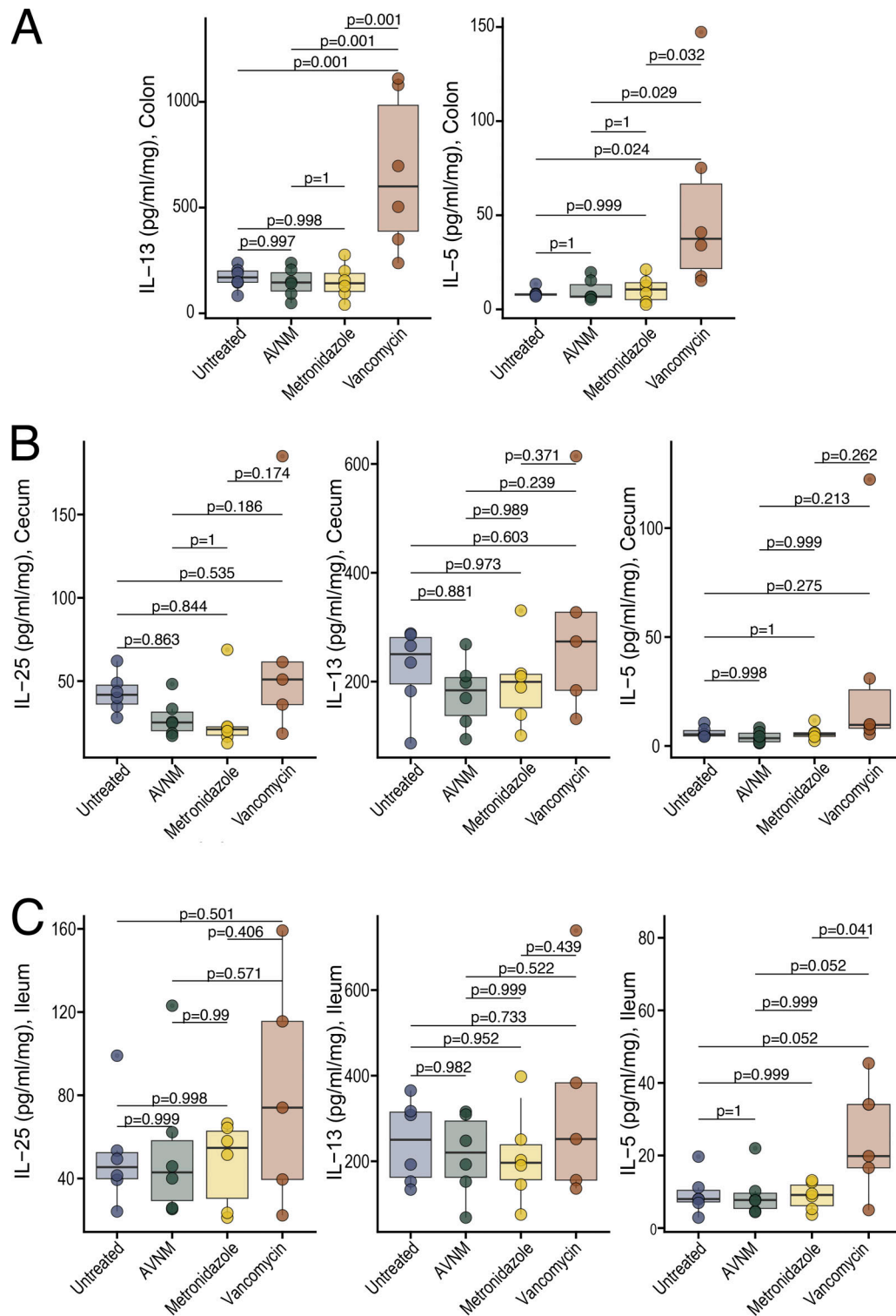


Figure S1. The figure shows additional ELISA results from antibiotic administration, confirming increases in TC-associated cytokines in (A) the colon, but not in (B) the cecum or (C) the ileum.

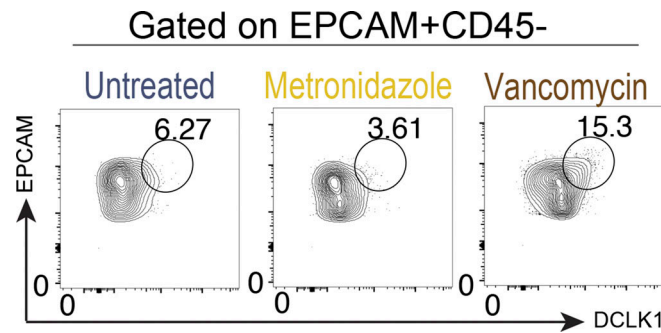


Figure S2. The figure shows the estimation of the percentage of TCs via flow cytometry by quantifying DCLK1+Epcam+ cells in mice treated with vancomycin, metronidazole, or PBS.

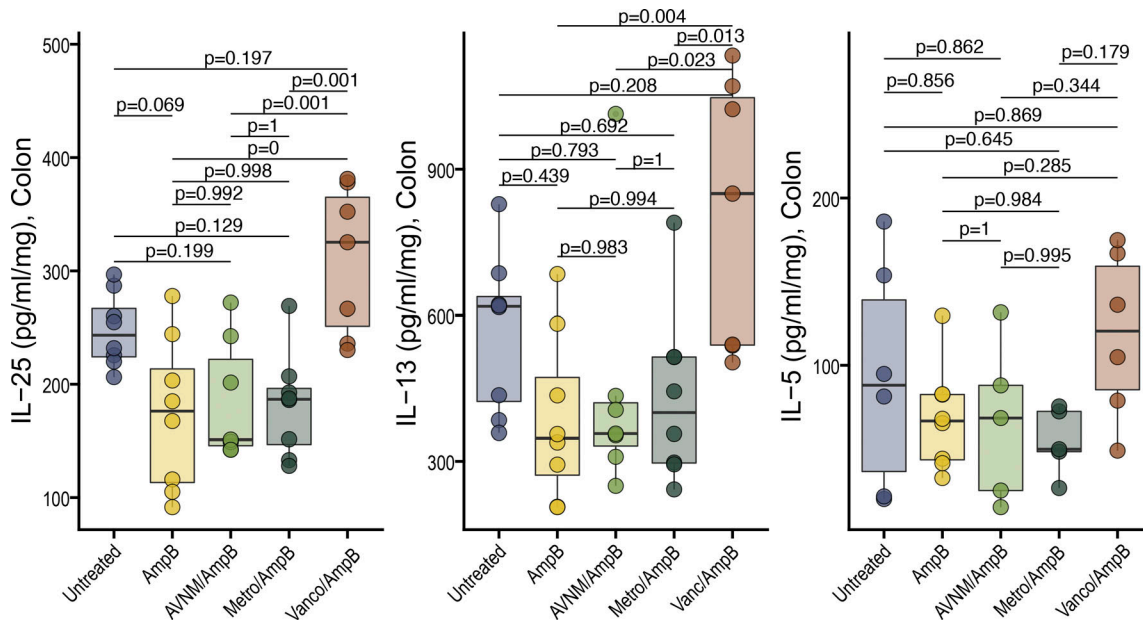


Figure S3. The figure reports the results from experiments showing that the antifungal amphotericin B does not change the ability of vancomycin to upregulate IL-25, IL5, and IL-13 in the proximal colon and confirms the bacterial role of this phenotype.

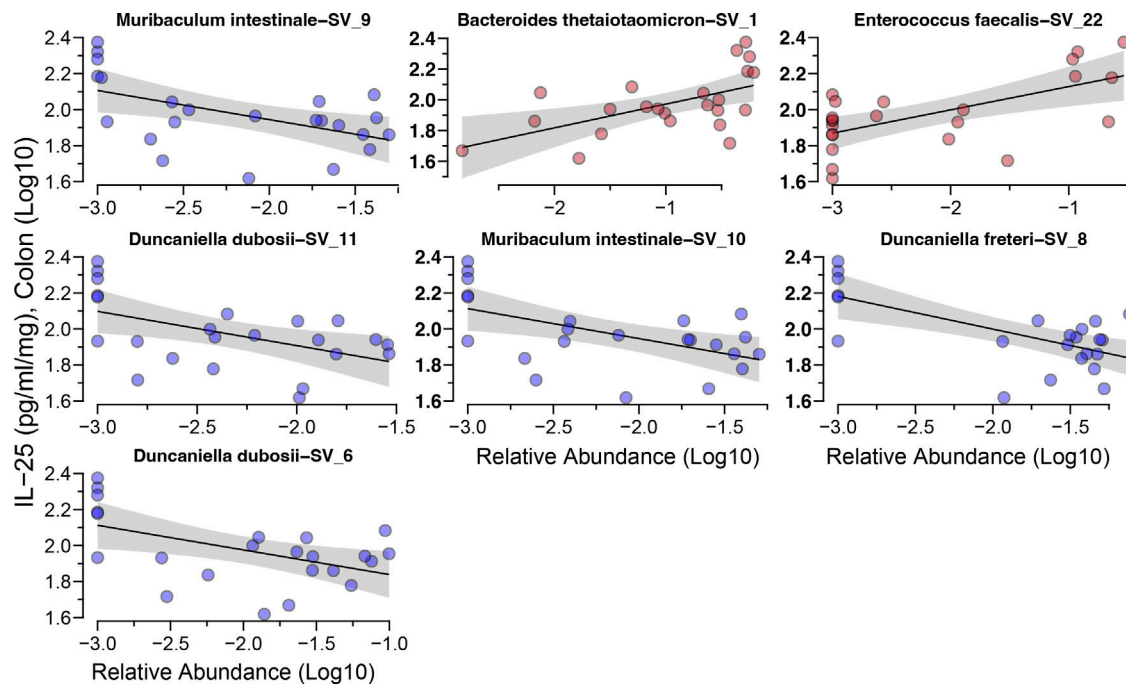


Figure S4. The figure reports Spearman's correlation analysis results between the relative abundance of microbiota amplicon SVs and colonic IL-25 in AVNM-treated animals receiving FMT from untreated or vancomycin-treated mice.

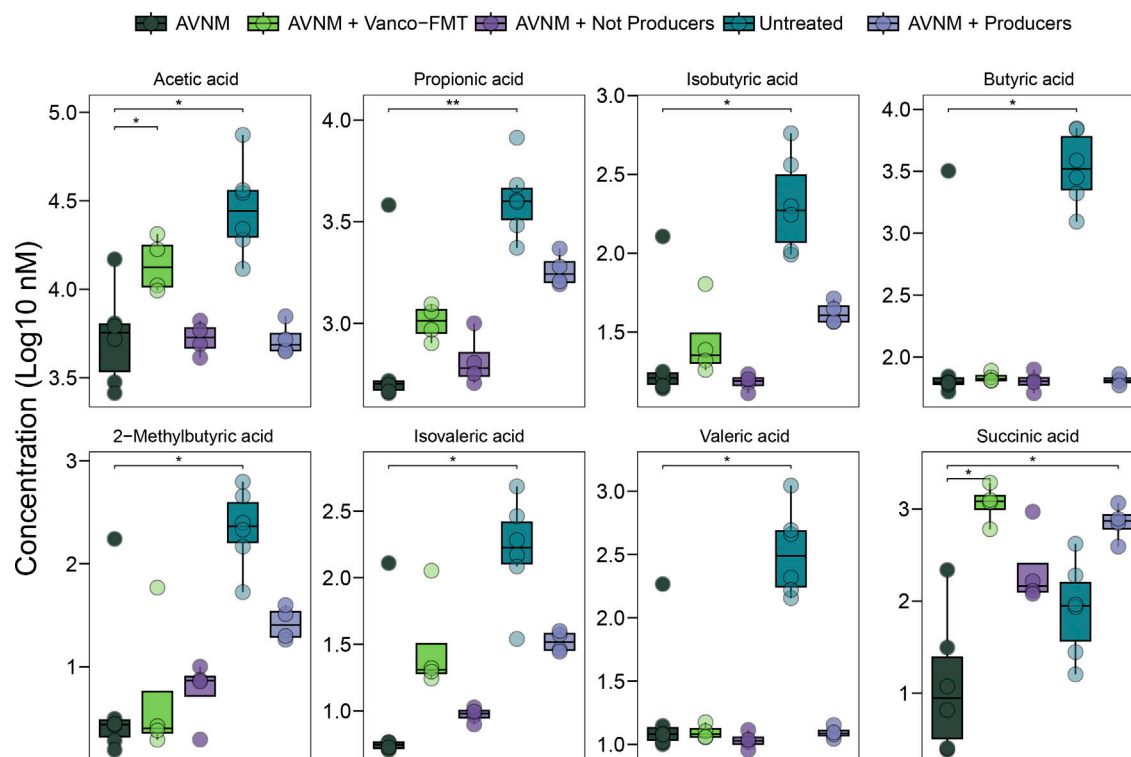


Figure S5. The figure reports the results from targeted metabolomics for succinate and SCFAs from feces of mice treated with FMTs, succinate-producing bacteria, non-succinate-producing bacteria, or PBS. * indicates FDR-adjusted P-value for ANOVA with Tukey post-hoc test <0.05.

Provided online is Table S1. Table S1 shows RT-qPCR primer sequences.